สัญญาเลขที่ R2560C089

รายงานวิจัยฉบับสมบูรณ์

การศึกษาและควบคุมการติดเชื้อของโรคอหิวาจากการแยกกลุ่มอายุคน

ผู้ช่วยศาสตราจารย์ ดร.ชัยรัตน์ มดนาค

ภาควิชาคณิตศาสตร์ คณะวิทยาศาสตร์

กองทุนวิจัยมหาวิทยาลัยนเรศวร

บทคัดย่อ

งานวิจัยนี้ได้ศึกษาเกี่ยวกับการระบาดของโรคอหิวาและการควบคุมโดยการพิจารณาแยกอายุกลุ่มคน ซึ่งแบบจำลองทางคณิตศาสตร์ที่ได้เป็นระบบสมการเชิงอนุพันธ์ย่อยสี่สมการในการอธิบายการระบาดของโรค โดยที่หนึ่งสมการเพิ่มเติมเป็นสมการเชิงอนุพันธ์สำหรับการเติบโตของแบคทีเรีย ความสมดุลของจุดวิกฤติได้รับการตรวจพิสูจน์และผลเฉลยเชิงตัวเลขถูกใช้เป็นเครื่องมือในการยืนยันผล โดยงานวิจัยนี้ได้ศึกษาต่อยอดโดยใช้ทฤษฎีควบคุมอย่างงเหมาะสม (optimal control theory) ในการหาแนวทางเพื่อป้องกัน ควบคุม และรักษาการติดเชื้อของโรคอหิวา ซึ่งงานวิจัยนี้มีประโยชน์สำหรับประเทศยากจนที่ไม่มีงบประมาณเพียงพอในการฉีดวัคซีนกับประชาชนในประเทศทั้งหมด นั่นคือองค์กรที่เกี่ยวข้องต้องมีการวางแผนควบคุมการระบาดโดยใช้แนวทางต่างๆควบคู่กันไปเชิงนโยบาย อย่างเช่น การบำบัดน้ำเสีย การรณรงค์ไม่ให้คนทิ้งเศษขยะลงแม่น้ำลำคลอง หรือการป้องกันการติดเชื้อโดยการรักษาสุขอนามัยให้อยู่ในเกณฑ์ที่ดี

คำสำคัญ : โรคอหิวา การรักษาด้วยการฉีดวัคซีน การหาค่าเหมาะสม การควบคุมโรค การแบ่งกลุ่มคน

Abstract

In this study, we formulate an age-structured cholera model with four partial differential equations describing the transmission dynamics of human hosts and one ordinary differential equation representing the bacterial evolution in the environment. We conduct rigorous analysis on the trivial (disease-free) and non-trivial (endemic) equilibria of the system, and establish their existence, uniqueness, and stability where possible. Meanwhile, we perform an optimal control study for the age-structured model and seek effective vaccination strategies that best balance the outcome of vaccination in reducing cholera infection and the associated costs. Our modeling, the human hosts with explicit age structure, and the age-dependent vaccination as a disease control measure.

Keyword: Cholera model, Disease control, Stability, Optimal control, Age-structured

Executive Summary

1. ความสำคัญและที่มาของปัญหาที่ทำการวิจัย

โรคอหิวาเป็นโรคร้ายแรง ผู้ติดเชื้อที่ปราศจากการรักษาอย่างถูกต้อง สามารถเสียชีวิตได้อย่างเฉียบพลัน การระบาดของโรคอหิวาเกิดได้หลายสาเหตุ อย่างเช่น การดื่มน้ำที่ปนเปื้อนเชื้อแบคทีเรียสายพันธ์ Vibrio Cholerae หรืออาหารดิบๆสุกๆซึ่งมีเชื้อแบคทีเรียสายพันธ์นี้ปนเปื้อน ส่วนการแพร่ระบาดของโรคจากคนสู่คนไม่ค่อยพบเห็นมากนัก

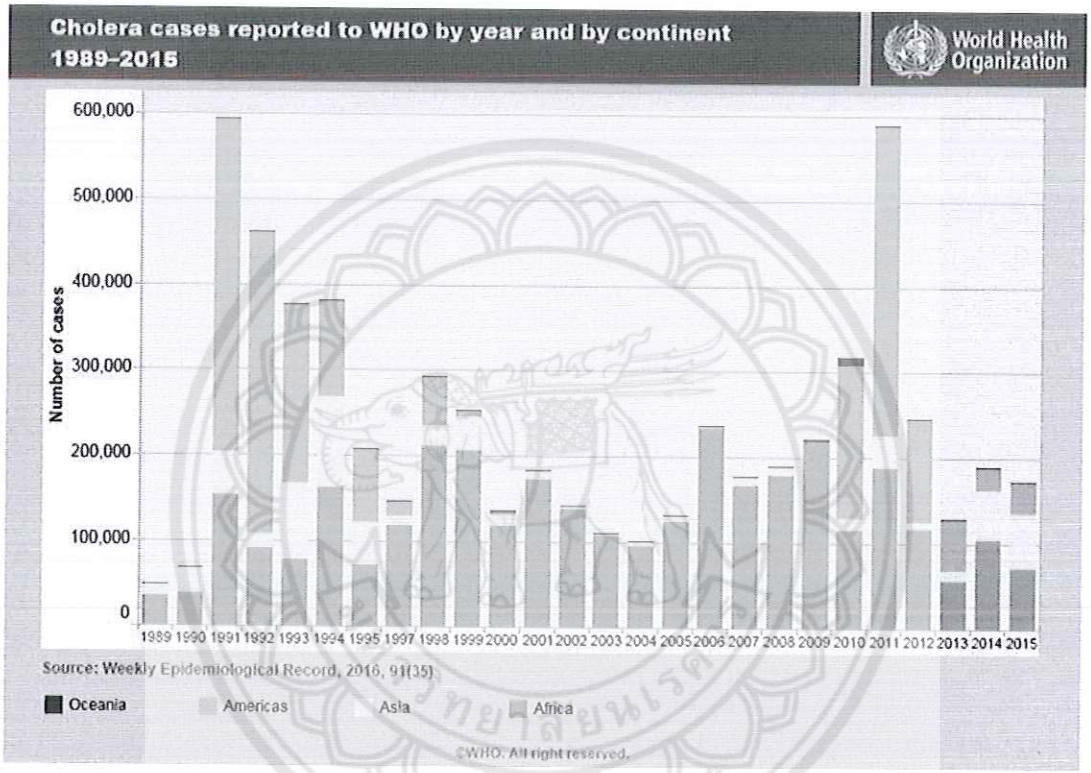

ไม่นานมานี้ เราจะเห็นว่ายังมีข่าวการแพร่ระบาดของโรคนี้ทั่วโลก และจะเห็นว่าจำนวนครั้งที่เกิดเพิ่มมากขึ้นทุกๆปี ครั้งล่าสุดในปี 2010-2011 ในประเทศ Haiti เป็นการกลับมาระบาดครั้งยิ่งใหญ่ของโรคนี้อีกครั้งในยุคสมัยใหม่นี้ และเป็นครั้งที่ร้ายแรงที่สุด โดยจากรายงานพบว่า มีผู้ติดเชื้อมากกว่า 530,000 ราย และเสียชีวิตมากกว่า 7,000 ราย [1] การระบาดของโรคครั้งสำคัญๆที่มีผู้เสียชีวิตเป็นจำนวนมากยังพบเห็นได้ในหลายประเทศ อาทิเช่น Sierra Leone ในปี 2012, Nigeria ในปี 2010, Vietnam ในปี 2009, Zimbabwe ในปี 2008 และประเทศอินเดียในปี 2007 สำหรับประเทศไทยยังพบผู้ติดเชื้อโรคอหิวาทุกปี โดยข้อมูลจากสำนักระบาดวิทยา กรมควบคุมโรค พบว่า ตั้งแต่วันที่ 1 มกราคม – 18 กันยายน 2555 ได้รับรายงานผู้ป่วยยืนยันอหิวาตกโรค จำนวน 29 ราย โดยมีรายงาน

จาก 10 จังหวัด ได้แก่ จังหวัดตาก 13 ราย ยะลา 5 ราย กรุงเทพ 4 ราย เชียงใหม่ ประจวบคีรีขันธ์ ตราด สุพรรณบุรี นครราชสีมา ภูเก็ต ระนอง จังหวัดละ 1 ราย [2]

มีการศึกษาโดยใช้แบบจำลองคณิตศาสตร์มากมายสำหรับโรคอหิวา เพื่อทำความเข้าใจเกี่ยวกับโรค พฤติกรรมของการแพร่ระบาดของโรค รวมทั้งการควบคุมการแพร่ระบาด ในปี 2009 Mukandavire [3] เสนอแบบจำลองทางคณิตศาสตร์ที่ไม่ซับซ้อนมากนัก ง่ายต่อการเข้าใจ และมีความซับซ้อนในการหาผลเฉลยทางตัวเลขน้อย ซึ่งเป็นแบบจำลองที่ผู้วิจัยมากมายนำไปต่อยอด โดยที่โมเดลคือ

$$\frac{dS}{dt} = \mu N - \beta_e S \frac{B}{k+B} - \beta_h SI - \mu S$$

$$\frac{dI}{dt} = \beta_e S \frac{B}{k+B} + \beta_h SI - (\gamma + \mu) I$$

$$\frac{dR}{dt} = \gamma I - \mu R$$

$$\frac{dB}{dt} = \varepsilon I - \delta B$$

โดยที่ S คือ กลุ่มสุ่มเสี่ยงของผู้ติดเชื่อ I คือ กลุ่มผู้ติดเชื้อ R คือ กลุ่มผู้ที่ได้รับการรักษาหายแล้ว และ B คือ กลุ่มประชากรของแบคทีเรีย โดยที่พารามิเตอร์อื่นๆคือค่าคงตัวต่างๆ

2. วัตถุประสงค์

เพื่อสร้างแบบจำลองทางคณิตศาสตร์ในการอธิบายการระบาดของโรคอหิวาโดยการศึกษาการแบ่งกลุ่มอายุของกลุ่มคน

3. ระเบียบวิธีวิจัย

3.1 ศึกษาแบบจำลองทางคณิตศาสตร์ต้นแบบที่นำเสนอโดย Mukandavire

3.2 ศึกษาแบบจำลองทางคณิตศาสตร์อื่นๆที่เกี่ยวข้องกับโรคอหิวาเพื่อเป็นประโยชน์ต่อการขยายโมเดล

3.3 สร้างแบบจำลองทางคณิตศาสตร์ขั้นสูงสำหรับโรคอหิวาโดยการแบ่งกลุ่มอายุของคน

3.4 ตรวจสอบความถูกต้องของโมเดล

3.5 ศึกษาความเป็นไปได้ในการขยายแบบจำลองทางคณิตศาสตร์เพื่องานวิจัยในอนาคตและการประยุกต์ใช้

3.6 สรุปและเขียนงานวิจัย เพื่อตีพิมพ์ในวารสารและรายงานไปยังเจ้าของทุนวิจัย

4. แผนการดำเนินงานวิจัย

กิจกรรม	เดือนที่											
	1	2	3	4	5	6	7	8	9	10	11	12
1. ศึกษาแบบจำลองทางคณิตศาสตร์ต้นแบบที่นำเสนอโดย Mukandavire												
2. ศึกษาแบบจำลองทางคณิตศาสตร์อื่นๆที่เกี่ยวข้องกับโรคอหิวาเพื่อเป็นประโยชน์ต่อการขยายโมเดล												
3. สร้างแบบจำลองทางคณิตศาสตร์ขั้นสูงสำหรับโรคอหิวาสำหรับการแบ่งกลุ่มอายุของคน และตรวจสอบความถูกต้อง												
4. ศึกษาความเป็นไปได้ในการขยายแบบจำลองทางคณิตศาสตร์เพื่องานวิจัยในอนาคตและการประยุกต์ใช้												
5. สรุปและเขียนงานวิจัย เพื่อตีพิมพ์ในวารสารและรายงานไปยังเจ้าของทุนวิจัย												

5. ตัวชี้วัดเพื่อการเมินผลสำเร็จของโครงการ

5.1 ตีพิมพ์ในวารสารระดับนานาชาติที่มีค่า Impact Factor **จำนวน 1 เรื่อง**

เนื้อหางานวิจัย

(ดูรายระเอียดทั้งหมดดังเอกสารแนบหน้าถัดไป)

LIST OF CONTENTS

Chapter 1

Introduction

Cholera is an acute enteric infection caused by the ingestion of bacterium Vibrio cholerae present in faecally contaminated water or food. Primarily linked to insufficient access to safe water and proper sanitation, its impact can be even more dramatic in areas where basic environmental infrastructures are disrupted or have been destroyed. Countries facing complex emergencies are particularly vulnerable to cholera outbreaks.

Massive displacement of IDPs or refugees to overcrowded settings, where the provision of potable water and sanitation is challenging, constitutes also a risk factor. In consequence, it is of paramount importance to be able to rely on accurate surveillance data to monitor the evolution of the outbreak and to put in place adequate intervention measures Coordination of the different sectors involved is essential, and WHO calls for the cooperation of all to limit the effect of cholera on populations.

Cholera is characterized in its most severe form by a sudden onset of acute watery diarrhoea that can lead to death by severe dehydration. The extremely short incubation period - two hours to five days - enhances the potentially explosive pattern of outbreaks, as the number of cases can rise very quickly. About 75% of people infected with cholera do not develop any symptoms. However, the pathogens stay in their faeces for 7 to 14 days and are shed back into the environment, possibly infecting other individuals. Cholera is an extremely virulent disease that affects both children and adults. Unlike other diarrhoeal diseases, it can kill healthy adults within hours. Individuals with lower immunity, such as malnourished children or people living with HIV, are at greater risk of death if infected by cholera.

1.1 THE CAUSE OF THE CHOLERA DISEASE

Vibrio cholerae, the bacterium that causes cholera, is usually found in food or water contaminated by feces from a person with the infection. Common sources include:

- Municipal water supplies.
- Ice made from municipal water.
- Foods and drinks sold by street vendors.
- Vegetables grown with water containing human wastes.

• Raw or undercooked fish and seafood caught in waters polluted with sewage.

When a person consumes the contaminated food or water, the bacteria release a toxin in the intestines that produces severe diarrhea.It is not likely you will catch cholera just from casual contact with an infected person.

1.2 SYMPTOMS

Cholera is an extremely virulent disease that can cause severe acute watery diarrhoea. It takes between 12 hours and 5 days for a person to show symptoms after ingesting contaminated food or water. Cholera affects both children and adults and can kill within hours if untreated.

Most people infected with V. cholerae do not develop any symptoms, although the bacteria are present in their faeces for 1-10 days after infection and are shed back into the environment, potentially infecting other people.

Among people who develop symptoms, the majority have mild or moderate symptoms, while a minority develop acute watery diarrhoea with severe dehydration. This can lead to death if left untreated.

1.3 TREATMENT

Cholera is an easily treatable disease. The majority of people can be treated successfully through prompt administration of oral rehydration solution (ORS). The WHO/UNICEF ORS standard sachet is dissolved in 1 litre (L) of clean water. Adult patients may require up to 6 L of ORS to treat moderate dehydration on the first day.

Severely dehydrated patients are at risk of shock and require the rapid administration of intravenous fluids. A 70 kg adult will require at least 7 L of intravenous fluid, plus ORS during their treatment. These patients are also given appropriate antibiotics to diminish the duration of diarrhoea, reduce the volume of rehydration fluids needed, and shorten the amount and duration of V. cholerae excretion in their stool.

Mass administration of antibiotics is not recommended, as it has no proven effect on the spread of cholera and contributes to increasing antimicrobial resistance.

Rapid access to treatment is essential during a cholera outbreak. Oral rehydration should be available in communities, in addition to larger centres that can provide intravenous fluids and 24 hour care. With early and proper treatment, the case fatality rate should remain below 1%.

1.4 PREVENTION

Measures for the prevention of cholera mostly consist of providing clean water and proper sanitation to populations who do not yet have access to basic services. Health education and good food hygiene are equally important. Communities should be reminded of basic hygienic behaviours, including the necessity of systematic hand-washing with soap after defecation and before handling food or eating, as well as safe preparation and conservation of food. Appropriate media, such as radio, television or newspapers should be involved in disseminating health education messages. Community and religious leaders should also be associated to social mobilization campaigns.

In addition, strengthening surveillance and early warning greatly helps in detecting the first cases and put in place control measures. Conversely, routine treatment of a community with antibiotics, or mass chemoprophylaxis, has no effect on the spread of cholera, can have adverse effects by increasing antimicrobial resistance and provides a false sense of security.

Chapter 2

Basic Concepts

In this chapter, we will present some interesting mathematical models that describes the cholera dynamics. We will start with an early compartmental model that includes only a few state equations. The more complicated cholera model then will be studied. Finally, we will present and carefully study our model. Then, we will extend the model and explore strategies to control an cholera outbreak.

2.1 C. T. Codeco [2]

The model proposed here is an extension of Capasso's model , used to describe the 1973's cholera epidemics in Italy. In Capasso's version, two equations describe the dynamics of infected people in the community and the dynamics of the aquatic population of pathogenic bacteria. In our formulation, the dynamics of the susceptible population is included since I wish to study long term dynamics . The mathematical model is :

$$\begin{aligned} \frac{dS}{dt} &= n(H-S) - a\lambda(B)S, \\ \frac{dI}{dt} &= a\lambda(B)S - \gamma I, \\ \frac{dB}{dt} &= B(nb-mb) + eI, \end{aligned}$$

The diagram of this model is represented as follows:

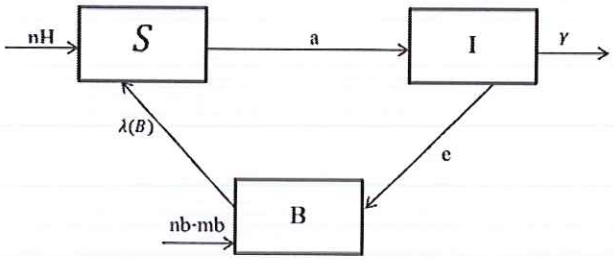

Figure 2.1: SIBS

Table 1 Biological meaning of all parameters and state variables

Parameter	Biological meaning
H	Total human population
n	Human birth and death rates (day^{-1})
a	Rate of exposure to contaminated water (day^{-1})
k	Concentration of V. cholerae in water that yields 50% chance of catching cholera (cells/ml)
r	Rate at which people recover from cholera (day^{-1})
nb	Growth rate of V. cholerae in the aquatic environment (day^{-1})
mb	Loss rate of V. cholerae in the aquatic environment (day^{-1})
e	Contribution of each infected person to the population of V. cholerae in the aquatic environment $(cell/ml day^{-1} person^{-1})$

2.2 D. M. Hartley, J. G. Morris Jr. and D. L. [4]

We have extended the Codeço model to incorporate a state of hyperinfectivity. In this modified model, infections(I) are caused by ingesting water contaminated with B_HHI vibrios per ml or B_L non-HI vibrios per ml. Ingestion of HI vibrios occurs at the rate β_H while ingestion of non-HI vibrios occurs at the rate β_L.When B_H equals κH, the probability of ingestion resulting in disease is 0.5, and similarly for B_L and κL.In other words, the models assume that the relationship between infection rates and the density of cholera is described by a saturating function $\frac{\beta B}{B+\kappa}$.Vibrios in the HI state decay into a state of lower infectivity ("non-HI") at the rate χ. Cases shed HI $V.cholerae$ into the aquatic environment at a rate ξ and cases cease to be infectious at the rate γ.Non-HI vibrios shed into the aquatic environment lose viability at the rate δL.These ideas are expressed in terms of the following set of differential equations:

$$
\begin{aligned}
\frac{dS}{dt} &= bN - \beta_L \frac{B_L}{\kappa_L + B_L} - \beta_H S \frac{B_H}{\kappa_H + B_H}, \\
\frac{dI}{dt} &= \beta_L \frac{B_L}{\kappa_L + B_L} + \beta_H S \frac{B_H}{\kappa_H + B_H} - (\gamma + b)I, \\
\frac{dR}{dt} &= \gamma I - bR, \\
\frac{dB_H}{dt} &= \xi I - \chi B_H, \\
\frac{dB_L}{dt} &= \chi B_H - \delta_L B_L,
\end{aligned}
$$

The diagram of this model is represented as follows:

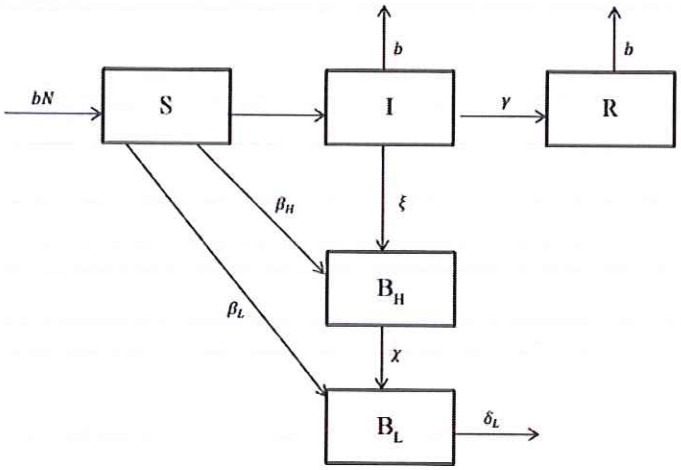

Figure 2.2: SIRB.

Table 2 Biological meaning of all parameters

Parameter	Biological meaning
β_L	Rate of drinking LI $V.cholerae$
β_H	Rate of drinking HI $V.cholerae$
κ_L	Non-HI $V.cholerae$ infectious concentration (IC_{50})
κ_H	HI $V.cholerae$ infectious concentration (IC_{50})
b	Natural human birth and death rate
χ	Rate of decay from hyper-to reduced infectiousness
ξ	Rate of contribution to HI $V.cholerae$ in aquatic environment
δ_L	Net death rate of non-HI vibrios in the environment
γ	Rate of recovery from cholera

2.3 J. Wang, C. Modnak : [6]

Let $S(t)$, $I(t)$ and $R(t)$ denote the susceptible, the infected, and the recovered human population sets, respectively. The total population $N = S + I + R$ is assumed to be a constant, which is a reasonable assumption for a relatively short period of time and for low-mortality diseases such as cholera. Let also B denote the concentration of the vibrios in the environment (e.g., contaminated water). The cholera model developed in is a combined system of human populations and the environmental component $(SIR - B)$, with the environment-to-human transmission represented by a logistic (or, Michaelis-Menten type) function and the human-to-human transmission by the standard mass action law. We now extend this model by adding vaccination, treatment and water sanitation. We assume these controls are implemented continuously; specifically, we make the following assumptions:

• Vaccination is introduced to the susceptible population at a rate of $\nu(t)$, so that $\nu(t)S(t)$ individuals per time are removed from the susceptible class and added to the recovered class.

•Therapeutic treatment is applied to the infected people at a rate of $a(t)$, so that $a(t)I(t)$ individuals per time are removed from the infected class and added to the recovered class.

• Water sanitation leads to the death of vibrios at a rate of $\omega(t)$.

As a result, we obtain the following dynamical system:

$$\begin{aligned}
\frac{dS}{dt} &= \mu N - \beta_e S\frac{B}{\kappa + B} - \beta_h SI - \mu s - \nu(t)S, \\
\frac{dI}{dt} &= \beta_e S\frac{B}{\kappa + B} + \beta_h SI - (\gamma + \mu)I - a(t)I, \\
\frac{dB}{dt} &= \xi I - \delta B - \omega(t)B, \\
\frac{dR}{dt} &= \gamma I - \mu R + a(t)I + \nu(t)S,
\end{aligned}$$

The diagram of this model is represented as follows:

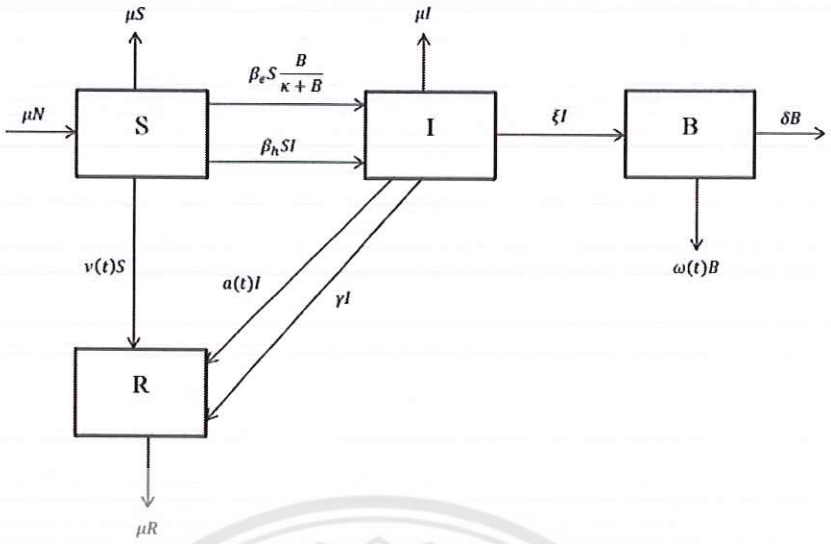

Figure 2.3: SIRB.

Table 3 Biological meaning of all parameters

Parameter	Biological meaning
N	Total population
μ	Natural human birth and death rate
κ	Concentration of $V.cholerae$ in environment
γ	Rate of recovery from cholera
ξ	Rate of human contribution to $V.cholerae$
δ	Death rate of vibrios in the environment
β_e	Ingestion rate from the environment
β_h	Ingestion rate through human-human interaction

Theorem 2.1. *(STABILITY PROPERTIES OF A LINEAR SYSTEM)*
Consider the linear system (3.19)*, and for each eigenvalue* λ *of* A*, suppose that* m_λ *denotes the algebraic multiplicity of* λ *and* d_λ *the geometric multiplicity of* λ*.*
Then :

(a) The system is asymptotically stable if and only if A is a **stability matrix;** *that is, every eigenvalue of A has a negative real part.*

(b) The system is neutrally stable if and only if

- *every eigenvalue of A has a nonpositive real part, and*

- *at least one eigenvalue has a zero real part, and $d_\lambda = m_\lambda$ for every eigenvalue λ with a zero real part.*

(c) The system is unstable if and only if

- *some eigenvalue of A has a positive real part, or*
- *there is an eigenvalue λ with a zero real part and $d_\lambda < m_\lambda$.*

NOTE : (1) Suppose all the eigenvalues of A have nonpositive real parts. One can prove that if all eigenvalues having zero real parts are distinct, then the origin is neutrally stabel. (2) Also, if every eigenvalue of A has a positive real part, then the system is completely unstable.

Proposition 2.2. *(THE ROUTH TEST) All the roots of the polynomial $a(\lambda)$ (with real coefficients) have negative real parts precisely when the given conditions are met.*

- $\lambda^2 + a_1\lambda + a_2$ *: all the coefficients are positive ;*
- $\lambda^3 + a_1\lambda^2 + a_2\lambda + a_3$ *: all the coeffients are positive and $a_1a_2 > a_3$;*
- $\lambda^4 + a_1\lambda^3 + a_2\lambda^2 + a_3\lambda + a_4$ *: all the coefficients are positive, $a_1a_2 > a_3$ and $a_1a_2a_3 > {a_1}^2a_4 + {a_3}^2$.*

Chapter 3

Mathematical Model

3.1 Our proposed model

As a start, we develop a PDE-ODE coupling system to describe the age-dependent cholera dynamics. We assume that the total human population is divided into four classes: susceptible, infected, vaccinated, and recovered. Let $S(a,t), I(a,t), V(a,t), R(a,t)$ denote, respectively, the number of susceptible, infected, vaccinated, and recovered humans at age a and time t. Let $B(t)$ be the concentration of vibrios in the contaminated environment at time t. We employ a saturation incidence in the form of $\beta(a)\frac{B(t)}{B(t)+\kappa}$ to model the force of infection from the environment, where κ is the half saturation concentration of environmental vibrios. Susceptible individuals become infected as a result of ingesting bacteria at rate $\beta(a)$. Moreover, $\mu(a)$ is the natural mortality rate. We further assume that susceptible individuals are vaccinated at an age-specific rate $\omega(t)$, with a vaccine efficacy $1-\sigma$ (we assume that the parameter σ is independent of age). Infected individuals are treated and subsequently enter the recovered class at a rate $\gamma(a)$. Infected individuals contribute to vibrios in the aquatic environment at an age-dependent rate $\alpha(a)$ and virbios have a reduction rate μ_b which includes the natural death and other means of the removal of the pathogen in the environment. Since the case fatality rates for cholera generally are very low (at or below 1%), we assume that the cholera-induced mortality can be neglected in this study. All these parameters take positive values.

Based on these assumptions, the dynamics of the disease transmission are described by the following equations:

$$\frac{\partial S}{\partial a}+\frac{\partial S}{\partial t}=-\beta(a)\frac{B(t)}{B(t)+\kappa}S(a,t)-(\omega(a)+\mu(a))S(a,t), \tag{3.1}$$

$$\frac{\partial I}{\partial a}+\frac{\partial I}{\partial t}=\beta(a)\frac{B(t)}{B(t)+\kappa}(S(a,t)+\sigma V(a,t))-(\gamma(a)+\mu(a))I(a,t), \tag{3.2}$$

$$\frac{\partial V}{\partial a}+\frac{\partial V}{\partial t}=\omega(a)S(a,t)-\sigma\beta(a)\frac{B(t)}{B(t)+\kappa}V(a,t)-\mu(a)V(a,t), \tag{3.3}$$

$$\frac{\partial R}{\partial a}+\frac{\partial R}{\partial t}=\gamma(a)I(a,t)-\mu(a)R(a,t), \tag{3.4}$$

$$\frac{dB(t)}{dt}=\int_0^\infty \alpha(a)I(a,t)da-\mu_b(t)B(t). \tag{3.5}$$

Cholera does not transmit vertically from mothers to children and newborns will appear in the recovered class. Thus, we choose the following non-negative initial and boundary conditions for our system:

$$S(0,t)=I(0,t)=V(0,t)=0, R(0,t)=\int_0^i nfb(a)(S(a,t)+I(a,t)+R(a,t)+V(a,t))da;$$
$$S(a,0)=S_0(a), I(a,0)=I_0(a), V(a,0)=V_0(a), R(a,0)=R_0(a), B(0)=B_0, \tag{3.6}$$

where $b(a)$ is the fecundity function. The initial age distributions are assumed to be known, and their values become zero beyond some maximum age.

Let $P(a,t)=S(a,t)+I(a,t)+R(a,t)+V(a,t)$. It is straightforward to observe that

$$\frac{\partial P}{\partial a}+\frac{\partial P}{\partial t}=-\mu(a)P(a,t), \tag{3.7}$$

$$P(0,t)=\int_0^\infty b(a)P(a,t)da, \tag{3.8}$$

$$P(a,0)=P_0(a), \tag{3.9}$$

where $P_0(a)=S_0(a)+I_0(a)+R_0(a)+V_0(a)$. Further, let $b_0=\int_0^i nfb(a)P_0(a)da$. As $t\to\infty$,

$$P(a,t)\to b_0 exp-\int_0^a \mu(\tau)d\tau =: P_\infty(a).$$

Set

$$s(a,t)=\frac{S(a,t)}{P_\infty(a)}, i(a,t)=\frac{I(a,t)}{P_\infty(a)}, v(a,t)=\frac{V(a,t)}{P_\infty(a)}.$$

The original system can then be reduced to the following

$$\begin{aligned}
\frac{\partial s}{\partial a}+\frac{\partial s}{\partial t} &= -\beta(a)\frac{B(t)}{B(t)+\kappa}s(a,t)-(\omega(a)+\mu(a))s(a,t),\\
\frac{\partial i}{\partial a}+\frac{\partial i}{\partial t} &= \beta(a)\frac{B(t)}{B(t)+\kappa}(s(a,t)+\sigma v(a,t))-\gamma(a)i(a,t), \qquad (3.10)\\
\frac{\partial v}{\partial a}+\frac{\partial v}{\partial t} &= \omega(a)s(a,t)-\sigma\beta(a)\frac{B(t)}{B(t)+\kappa}v(a,t),\\
\frac{\partial R}{\partial a}+\frac{\partial R}{\partial t} &= \gamma(a)I(a,t)-\mu(a)R(a,t), \qquad (3.11)\\
\frac{dB(t)}{dt} &= \int_0^\infty \alpha(a)i(a,t)P_\infty(a)da-\mu_b(t)B(t).
\end{aligned}$$

The model (3.10) with the initial and boundary conditions is well-posed.

We proceed to analyze the dynamics of our cholera model described in system (3.10). For ease of presentation, we let $\kappa = 1$ (through a normalization) in this section. Introduce

$$\mathbb{F}_\omega(a) = exp\{-\int_0^a \omega(\tau)d\tau\}.$$

It is easy to obtain that

$$E_0(s^0(a), i^0(a), v^0(a), B^0) = (\mathbb{F}_\omega(a), 0, \int_0^a \omega(\zeta)\mathbb{F}_\omega(\zeta)d\zeta, 0) \qquad (3.12)$$

is the disease-free (or, infection-free) equilibrium of the system.

To investigate the stability of the steady-state age distributions, we write

$$\begin{aligned}
s(a,t) = s^0(a)+\tilde{s}(a,t), i(a,t) = i^0(a)+\tilde{i}(a,t),\\
v(a,t) = v^0(a)+\tilde{v}(a,t), B(t) = B^0+\tilde{B}(t), \qquad (3.13)
\end{aligned}$$

for some small perturbations $\tilde{s}, \tilde{i}, \tilde{v}$ and $\tilde{B}$. Substitute these into our system, we obtain

$$\frac{\partial \tilde{s}(a,t)}{\partial a}+\frac{\tilde{s}(a,t)}{\partial t} = -\beta(a)\Big(\frac{B^0}{B^0+1}\tilde{s}(a,t)+\frac{1}{(B^0+1)^2 s^0(a)\tilde{B}(t)}\Big)-\omega(a)\tilde{s}(a,t), \qquad (3.14)$$

$$\frac{\partial \tilde{i}(a,t)}{\partial a}+\frac{\tilde{i}(a,t)}{\partial t} = \beta(a)\frac{B^0}{B^0+1}(\tilde{s}(a,t)+\sigma\tilde{v}(a,t))+\beta(a)\frac{B^0}{(B^0+1)^2}(\tilde{s^0}(a,t)+\sigma\tilde{v^0}(a,t))\tilde{B}(t)- \qquad (3.15)$$

$$\frac{\partial \tilde{v}(a,t)}{\partial a}+\frac{\tilde{v}(a,t)}{\partial t} = \omega(a)\tilde{s}(a,t)-\sigma\beta(a)\Big(\frac{B^0}{B^0+1}\tilde{v}(a,t)+\frac{1}{(B^0+1)^2}s^0(a)\tilde{B}(t)\Big), \qquad (3.16)$$

$$\frac{d\tilde{B}(t)}{dt} = \int_0^\infty \alpha(a)\tilde{i}(a,t)P_\infty(a)da-\mu_b\tilde{B}, \qquad (3.17)$$

with the initial and boundary conditions

$$\tilde{s}(a,0) = s_0(a) - s^0(a), \tilde{i}(a,0) = i_0(a) - i^0(a), \tilde{v}(a,0) = v_0(a) - v^0(a),$$
$$\tilde{B}(0) = B_0 - B^0, \tilde{s}(0,t) = \tilde{i}(0,t) = \tilde{v}(0,t) = 0.$$

3.2 Optimal treatments

In this section, we will use the following theorem to apply optimal control theory to seek cost effective treatment programs for our model.

Pontryagin's Maximum Principle

These conclusions can be extended to a version of Pontryagin's Maximum Principle.

Theorem 3.1. *If $u^*(t)$ and $x^*(t)$ are optimal for problem (3.1)-(3.6), then there exists a piecewise differentiable adjoint variable $\lambda(t)$ such that*

$$H(t, x^*(t), u(t), \lambda(t)) \leq H(t, x^*(t), u^*(t), \lambda(t))$$

for all control u at each time t, where the Hamiltonian H is

$$H = f(t, x(t), u(t)) + \lambda(t) g(t, x(t), u(t)),$$

and

$$\lambda'(t) = -\frac{\partial H(t, x^*(t), u^*(t), \lambda(t))}{\partial x}, \lambda(t_1) = 0.$$

Theorem 3.2. *Suppose that $f(t,x,u)$ and $g(t,x,u)$ are both continuously differentiable functions in thier three arguments and concave in u. Suppose u^* is an optimal control for problem (3.1)-(3.6), with associated state x^*, and λ a piecewise differentiable function with $\lambda \geq 0$ for all t. Suppose for all $t_0 \leq t \leq t_1$*

$$0 = H_u(t, x^*(t), u^*(t), \lambda(t)).$$

Then for all controls u and each $t_0 \leq t \leq t_1$, we have

$$H(t, x^*(t), u(t), \lambda(t)) \leq H(t, x^*(t), u^*(t), \lambda(t)).$$

In this section, we extend our study to an age-structure model to investigate the impact of different ages on cholera dynamics and the corresponding control strategy as follows:

$$\frac{\partial S}{\partial t} + \alpha_1 \frac{\partial S}{\partial a} = -\beta(a)\frac{B(t)}{B(t)+\kappa}S(a,t) - (\phi(a,t)+\mu(a))S(a,t), \quad (3.18)$$

$$\frac{\partial V}{\partial t} + \alpha_1 \frac{\partial V}{\partial a} = \phi(a,t)S(a,t) - \sigma\beta(a)\frac{B(t)}{B(t)+\kappa}V(a,t) - \mu(a)V(a,t), \quad (3.19)$$

$$\frac{\partial I}{\partial t} + \alpha_1 \frac{\partial I}{\partial a} = \beta(a)\frac{B(t)}{B(t)+\kappa}(S(a,t)+\sigma V(a,t)) - (\gamma(a)+\mu(a))I(a,t), \quad (3.20)$$

$$\frac{\partial R}{\partial t} + \alpha_1 \frac{\partial R}{\partial a} = \gamma(a)I(a,t) - \mu(a)R(a,t), \quad (3.21)$$

$$\frac{dB(t)}{dt} = \int_0^\infty \alpha(a)I(a,t)da - \mu_b(t)B(t) \quad (3.22)$$

where initial conditions are

$$\begin{aligned} S(n,0) &= S_0(a) \geq 0; n = 1,2,\cdots,A, \\ V(n,0) &= V_0(a) \geq 0; n = 1,2,\cdots,A, \\ I(n,0) &= I_0(a) \geq 0; n = 1,2,\cdots,A, \\ R(n,0) &= R_0(a) \geq 0; n = 1,2,\cdots,A, \\ B(0) &= B_0(t) \geq 0; t \in (0,T). \end{aligned}$$

and boundary conditions of the system are

$$\begin{aligned} S(0,t) &= 0; 0 \leq t \leq T, \\ V(0,t) &= 0; 0 \leq t \leq T, \\ I(0,t) &= 0; 0 \leq t \leq T, \\ R(0,t) &= \int_0^\infty b(a)(S(a,t)+I(a,t)+R(a,t)+V(a,t))da; 0 \leq t \leq T. \end{aligned}$$

The natural domain for this system is

$$\Omega = \{(a,t) | 0 \leq a \leq A, 0 \leq t \leq T\} \quad (3.23)$$

where $T > 0$ is the final time and $A > 0$ is the maximum age under consideration.

The presence of age-dependent control makes equilibrium analysis of the system (3.18)- (3.22) difficult, as the system becomes non-autonomous and the disease dynamics now depend on the control profile. We consider the system on a time interval $[0,T]$ for some $T > 0$. The control set is defined as

$$\Gamma = \{\phi(a,t) | 0 \leq \phi(a,t) \leq \phi_{max}\}, \quad (3.24)$$

where ϕ_{max} denotes the upper bound for the effort of vaccination. The bound reflects practical limitation on the maximum rate of control that can be implemented in a given time period.

We aim to minimize the total number of infections and the cost of control over the time interval $[0, T]$; i.e.,

$$\min_{\phi(a,t)\in\Gamma} \int_0^T \int_0^A (a_1(a)I(a,t) + a_2(a)\phi(a,t)S(a,t) + a_3(a)\phi^2(a,t))dadt \qquad (3.25)$$

where $a_1(a)$, $a_2(a)$ and $a_3(a)$ are appropriate cost parameters, generally depending on the age a. Quadratic terms are introduced to account for nonlinear costs potentially arising at high intervention level. The minimization process is subject to the partial differential equations in (3.18)-(3.22), which we now refer to as the state equations. Correspondingly, the unknowns S, V, I, R and B are now called the state variables, in contrast to the control variable ϕ. Our goal is then to determine the optimal control, $\phi^*(a,t)$, so as to minimize the objective functional in (3.25).

We first note that the control set Γ is closed and convex, and the integrand of the objective functional in (3.25) is also convex. Meanwhile, our model is linear in the control variable. Hence, based on the standard optimal control theorems, we obtain the following theorem.

Theorem 3.3. *There exists $\phi^*(a,t) \in \Gamma$ such that the objective functional in (3.25) is minimized.*

To proceed, we will use the Pontryagin's Maximum/Minimum Principle to seek the optimal control solution. This approach introduces the adjoint functions and represents an optimal control in terms of the state and adjoint functions, thus transferring the problem of minimizing the objective functional into minimizing the Hamiltonian with respect to the control.

We define the adjoint functions $\lambda_S, \lambda_V, \lambda_I, \lambda_R$, and λ_B associated with the state equations for S, V, I, R, and B, respectively. We then form the Hamiltonian, H, by multiplying each adjoint function with the right-hand side of its corresponding state equation, and adding each of these products to the integrand of the objective functional. As a

result, we obtain

$$
\begin{aligned}
H(a,t) &= a_1(a)I(a,t) + a_2(a)\phi(a,t)S(a,t) + a_3(a)\phi^2(a,t) && (3.26)\\
&+\lambda_S\Big[-\beta(a)\frac{B(t)}{B(t)+\kappa}S(a,t) - (\phi(a,t)+\mu(a))S(a,t)\Big] && (3.27)\\
&+\lambda_V\Big[\phi(a,t)S(a,t) - \sigma\beta(a)\frac{B(t)}{B(t)+\kappa}V(a,t) - \mu(a)V(a,t)\Big] && (3.28)\\
&+\lambda_I\Big[\beta(a)\frac{B(t)}{B(t)+\kappa}(S(a,t)+\sigma V(a,t)) - (\gamma(a)+\mu(a))I(a,t)\Big] && (3.29)\\
&+\lambda_R\Big[\gamma(a)I(a,t) - \mu(a)R(a,t)\Big] && (3.30)\\
&+\lambda_B\Big[\int_0^\infty \alpha(a)I(a,t)da - \mu_b(t)B(t)\Big]. && (3.31)
\end{aligned}
$$

To achieve the optimal control, the adjoint functions must satisfy

$$
\begin{aligned}
-((\lambda_S)_t + \alpha_1(\lambda_S)_a) &= \frac{\partial H}{\partial S}, && (3.32)\\
-((\lambda_V)_t + \alpha_1(\lambda_V)_a) &= \frac{\partial H}{\partial V}, && (3.33)\\
-((\lambda_I)_t + \alpha_1(\lambda_I)_a) &= \frac{\partial H}{\partial I}, && (3.34)\\
-((\lambda_R)_t + \alpha_1(\lambda_R)_a) &= \frac{\partial H}{\partial R}, && (3.35)\\
-\frac{d\lambda_B}{dt} &= \frac{\partial H}{\partial B}. && (3.36)
\end{aligned}
$$

These yield

$$
\begin{aligned}
-((\lambda_S)_t + \alpha_1(\lambda_S)_a) &= a_2(a)\phi(a,t) - \lambda_S(\beta(a)\frac{B(t)}{B(t)+\kappa} + (\phi(a,t)+\mu(a))) && (3.37)\\
&+\lambda_I\beta(a)\frac{B(t)}{B(t)+\kappa} + \lambda_V\phi(a,t) + \lambda_R(0,t)b(a), && (3.38)\\
-((\lambda_V)_t + \alpha_1(\lambda_V)_a) &= \lambda_I\beta(a)\frac{B(t)}{B(t)+\kappa}\sigma - \lambda_V(\sigma\beta(a)\frac{B(t)}{B(t)+\kappa} + \mu(a)) && (3.39)\\
&+\lambda_R(0,t)b(a), && (3.40)\\
-((\lambda_I)_t + \alpha_1(\lambda_I)_a) &= a_1(a) - \lambda_I(\gamma(a)+\mu(a)) + \lambda_R\gamma(a) && (3.41)\\
&+\lambda_R(0,t)b(a) + \lambda_B\alpha(a), && (3.42)\\
-((\lambda_R)_t + \alpha_1(\lambda_R)_a) &= -\lambda_R\mu(a) + \lambda_R(0,t)b(a), && (3.43)\\
\frac{d\lambda_B}{dt} &= \lambda_B\mu_b(t) + H(t)\int_0^A \beta(a)(\lambda_S S - \lambda_I(S+\sigma V) + \lambda_V\sigma V)da. && (3.44)
\end{aligned}
$$

where

$$H(t) = \frac{\kappa}{(B(t)+\kappa)^2}.$$

with boundary conditions

$$\lambda_S(a,T) = 0; \lambda_V(a,T) = 0,$$
$$\lambda_I(a,T) = 0; \lambda_R(a,T) = 0,$$

for $a \in (0, A)$ and

$$\lambda_S(A,t) = 0; \lambda_V(A,t) = 0,$$
$$\lambda_I(A,t) = 0; \lambda_R(A,t) = 0,$$
$$\lambda_B(T) = 0,$$

for $t \in (0, T)$ and where

$$b(a) = \begin{cases} \frac{1}{5}\sin^2\left(\left(\frac{a-15}{30}\right)\pi\right) & 15 < a < 45 \\ 0 & \text{otherwise} \end{cases}.$$

The characterization of the optimal control is

$$\phi^*(a,t) = \max[0, \min(\phi(a,t), \phi_{max})] \tag{3.45}$$

where

$$\phi(a,t) = \frac{(\lambda_S - \lambda_V - a_2(a))S(a,t)}{2a_3}. \tag{3.46}$$

and $\phi_{max} = 0.7$.

To summarize, our optimal control problem consists of the state system (3.18)-(3.22) with initial conditions, the adjoint equations (3.37)-(3.44) with the transversality conditions, and equation (3.45) to characterize the optimal control. Such a problem has to be solved numerically, we apply the forward finite difference in time and space to solve the state equations and backward in time and space to solve the adjoint equations in an iterative manner.

To carry out the numerical simulation, we list the values for various transmission rates in the state equations (3.18)-(3.22) in Table 3.1. We first assign the set of values (with appropriate units) to the cost parameters in (3.25) as $a_1 = 500, a_2 = 1$ and $a_3 = 1$. We also set the upper bound of the rate for vaccination $\phi_{max} = 0.7$.

Fig. 3.1(a) shows the total infection of all age curves for the model without vaccination (solid line), i.e., $\phi(a,t) = 0$, and that with the optimal vaccination implemented (dashed

line). We clearly see that the number of infections has been significantly reduced due to the vaccine. Fig. 3.1(b) and (c) show the infection curves of different ages for the model with vaccination control and without vaccination control, respectively; the results show age-dependent control has the impact in reducing number of infections. Fig. 3.1(d) and Fig. 3.2 show the profile of vaccination control in its optimal balance. We observe that the vaccination rate starts at its maximum value and remain at that level for a number of days before decreasing to lower levels of strength.

Table 3.1: Model parameters and values

Parameter	Symbol	Value
Maximum age	A	72
Mortality rate	μ	$0.01619/365$ /day
Ingesting vibrios rate	β	0.075 /day
Death rate for vibrios	μ_b	1/30 /day
Vaccine efficacy	$1-\sigma$	0.7
Rate of human contribution to V.*cholerae*	α	0.8 /day
Half saturation rate	κ	10^6 /day
Recovery rate	γ	1/5/day
Time	T	100 days
Age	A	72 years

Other parameter values are listed as follows: Ingesting vibrios rate age-dependent,

$$\beta(a) = 10 \times \begin{cases} 0 & 0 \le a \le 2 \\ 0.03a - 0.06 & 2 < a \le 7 \\ -0.0169a + 0.2683 & 7 < a \le 15 \\ 0.006a - 0.075 & 15 < a \le 25 \\ -0.0016a + 0.1152 & \text{otherwise} \end{cases} \tag{3.47}$$

and

$$S(a,0) = \begin{cases} 450a & 0 \le a \le 2 \\ -0.38198a^2 + 17.08376a + 867 & \text{otherwise} \end{cases} \tag{3.48}$$

with

$$I(a,0) = 0.02S(a,0)$$

and

$$B(0) = 0.001\kappa$$

.

As can be naturally expected, the cost of vaccination directly affect the strength and duration of the vaccination in its optimal balance. For demonstration, we now assume that the linear and quadratic capita costs for vaccination are increased to $a_2 = 100$ and $a_3 = 1000$. Fig. 3.3 (a) shows that the total number of infections for the model with vaccination is higher than that the previous set of cost parameters. Also, Fig.3.3 (d) shows the shorter duration of vaccination of all ages can be implemented compared to the previous set of cost parameters. In addition, some ages such as 50 and 60 years old cannot get vaccinated for this set of parameters; that is the vaccination rates for both ages are zeroes.

Now we turn to investigate only a higher quadratic cost parameter, i.e., we set $a_1 = 500, a_2 = 1$ and $a_3 = 100$. Fig. 3.8 shows that with higher quadratic cost, the duration of vaccination is shorter, however, due to small population, the total number of infectious looks the same as the first set of parameters.

In our simulations show that the cost parameters are related to the duration and strength of the vaccination control, however, in our numerical simulations we have assumed that the cost parameters are constants for all ages. In fact, in reality, costs could be varies for different ages which we hope to overcome this in our future work.

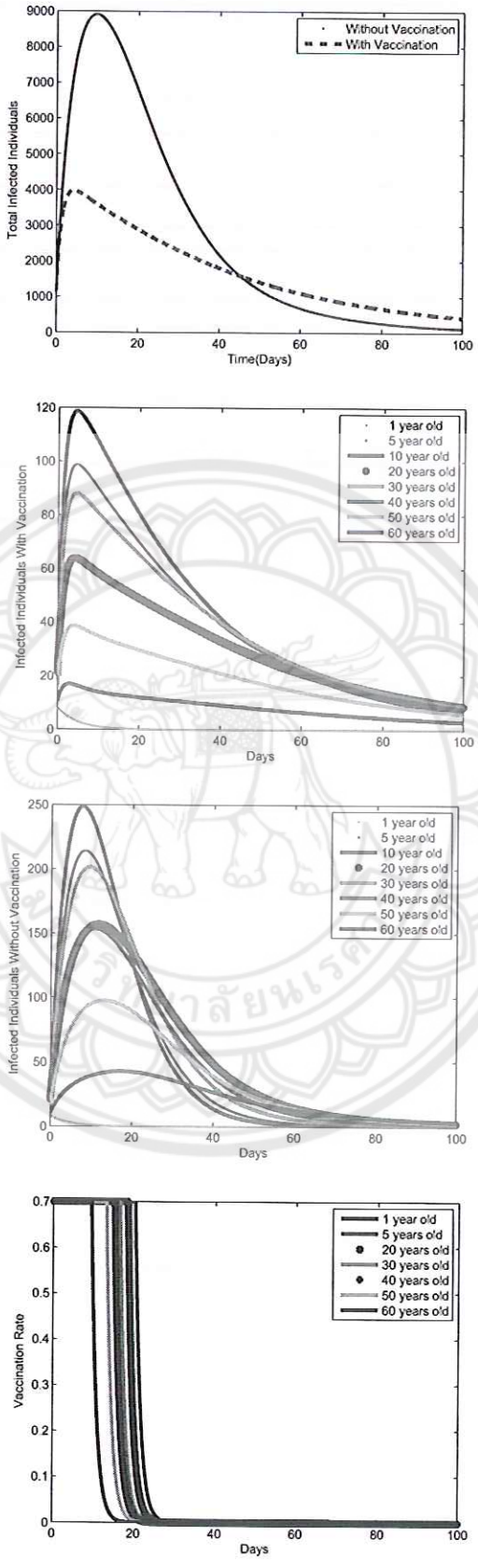

Figure 3.1: Optimal control simulation results based on the cost parameters $a_1 = 500, a_2 = 1$ and $a_3 = 1$: (a) Total infection curves for the cholera model with vaccination and without vaccination (b) infection curves with vaccination (c) infection curves

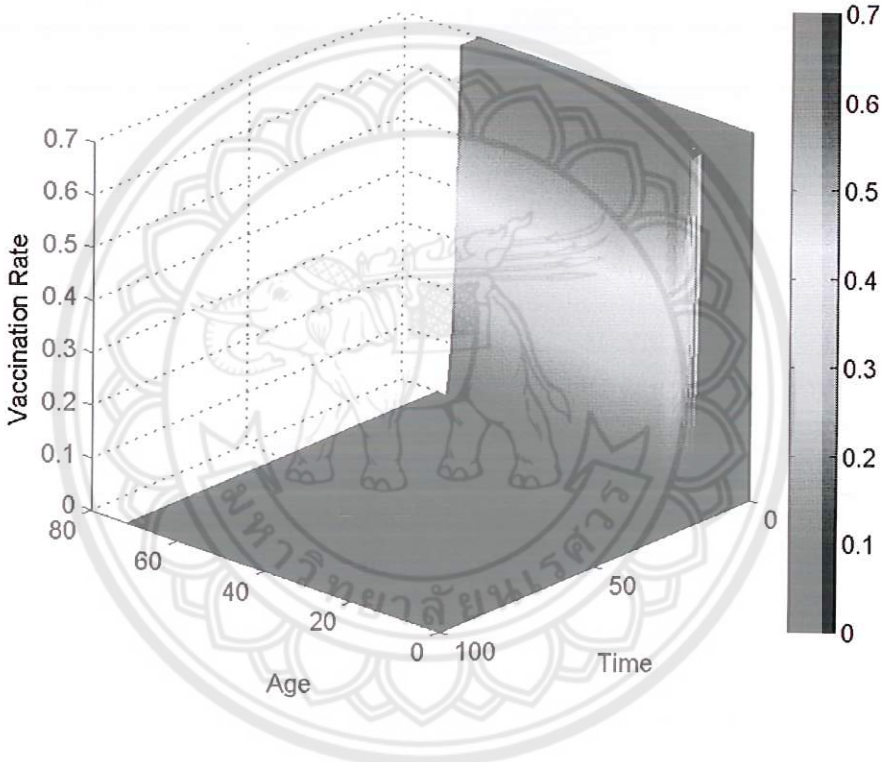

Figure 3.2: The three dimension plot of the optimal vaccination rates when the cost parameters are $a_1 = 500, a_2 = 1$ and $a_3 = 1$.

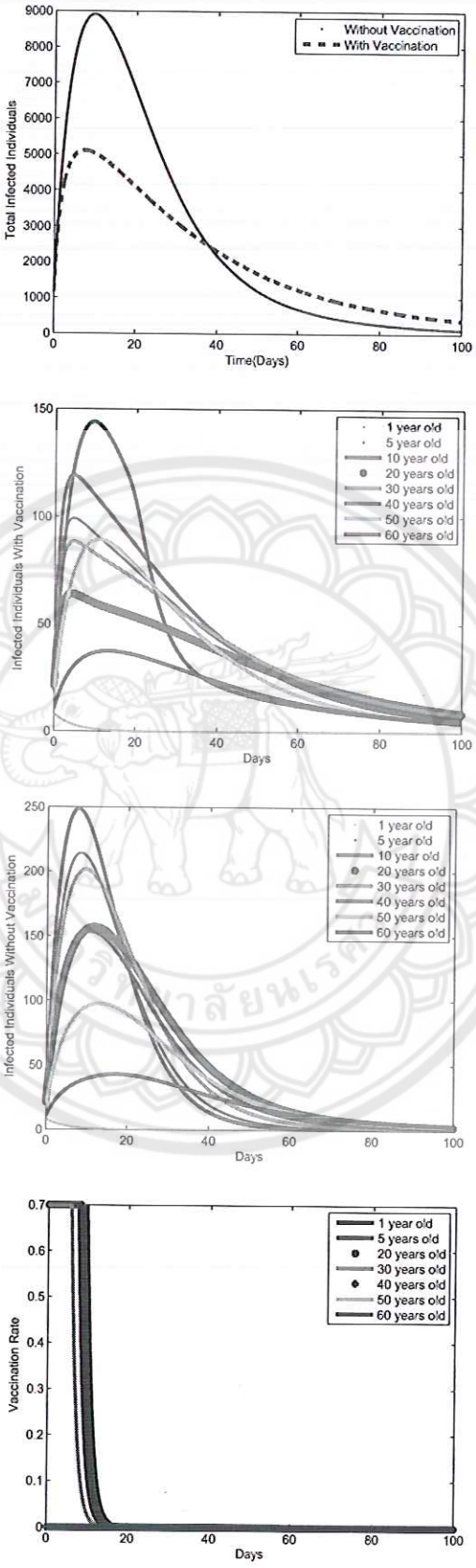

Figure 3.3: Optimal control simulation results based on the cost parameters $a_1 = 500, a_2 = 100$ and $a_3 = 1000$: (a) Total infection curves for the cholera model with vaccination and without vaccination (b) infection curves with vaccination (c) infection curves

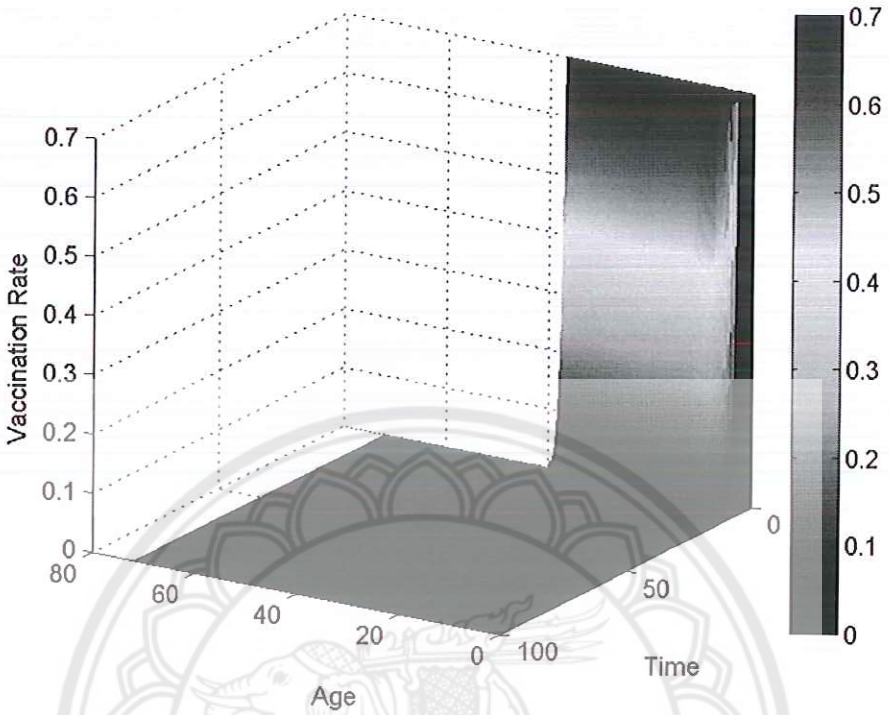

Figure 3.4: The three dimension plot of the optimal vaccination rates when the cost parameters are $a_1 = 500, a_2 = 100$ and $a_3 = 1000$.

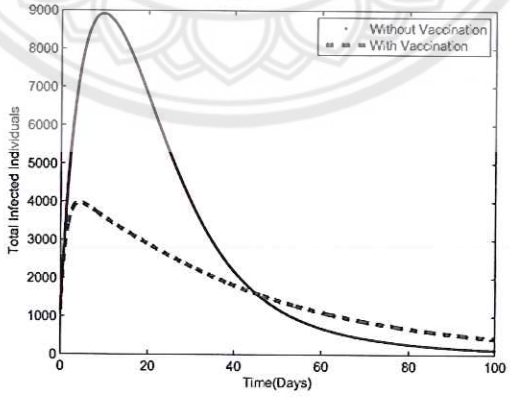

Figure 3.5: Optimal control simulation results based on the cost parameters $a_1 = 500, a_2 = 1$ and $a_3 = 100$: Total infection curves for the cholera model with vaccination and without vaccination

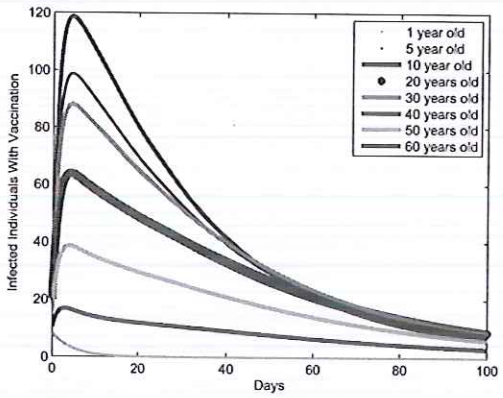

Figure 3.6: Optimal control simulation results based on the cost parameters $a_1 = 500, a_2 = 1$ and $a_3 = 100$: Infection curves with vaccination

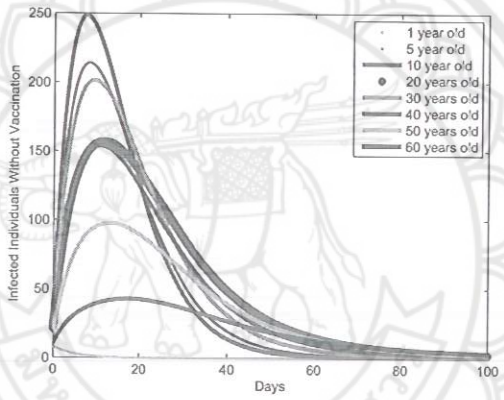

Figure 3.7: Optimal control simulation results based on the cost parameters $a_1 = 500, a_2 = 1$ and $a_3 = 100$:Infection curves without vaccination

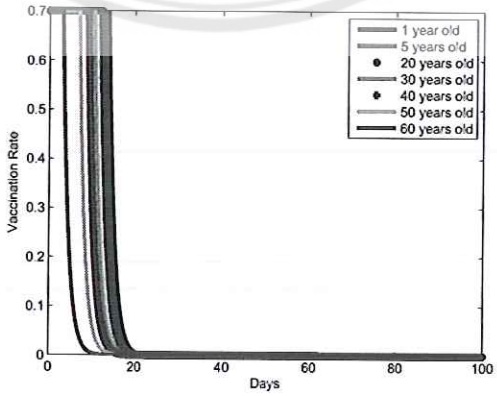

Figure 3.8: Optimal control simulation results based on the cost parameters $a_1 = 500, a_2 = 1$ and $a_3 = 100$: The optimal vaccination rates

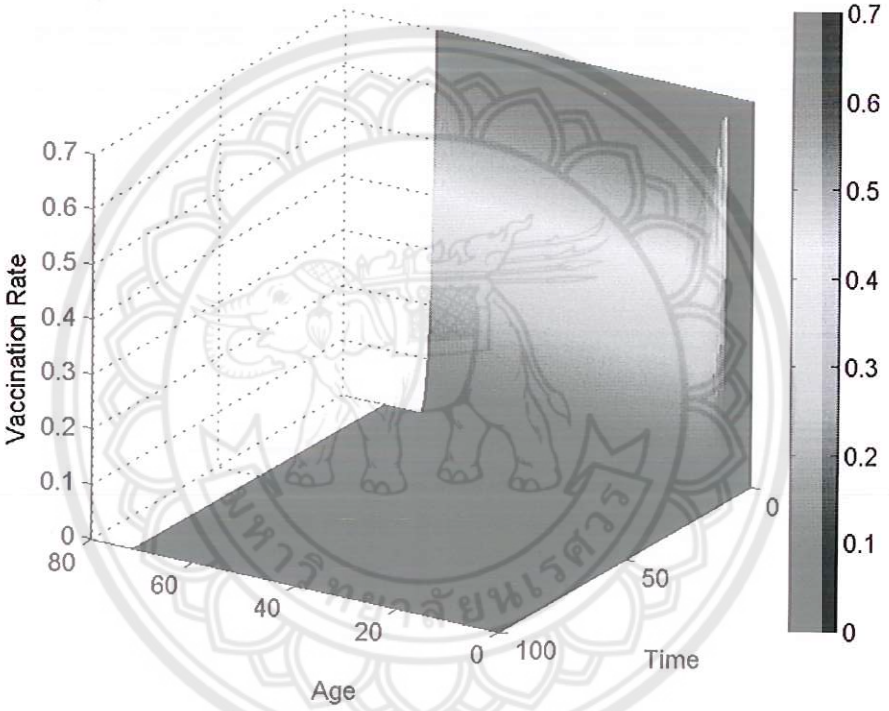

Figure 3.9: The three dimension plot of the optimal vaccination rates when the cost parameters are $a_1 = 500, a_2 = 1$ and $a_3 = 100$.

Chapter 4

Conclusions

In this paper, we have presented a mathematical model for control problem of cholera. We have studied in both theoretical and numerical ways, in order to observe the effect of rate of vaccination and the efficiency of other controls on the spread control of disease .

The model explains two feasible points of equilibrium, namely, the epidemic equilibrium and the endemic equilibrium. The stability of these two feasible points of equilibrium are controlled by the threshold number R_0. If R_0 is less than one, then the disease dies out and the epidemic equilibrium R_0 is stable. If R_0 is greater than one, then the disease persists and the disease free equilibrium is unstable. We have the values is based on the theory of R_0.

In addition, we have deployed controls to investigate strategies to reduce numbers of infectious CHOLERA people. The optimal control study is applied to seek numerical simulations along with analysis. The results show that with strategically deployed four controls; vaccination, treatment, sanitation and pesticide of flies, the number of infectious cholera prople can be reduced significantly.

REFERENCES

[1] B. Buonomo , *A simple analysis of vaccination strategies for Rubella*, Math. Biosci. Eng. 8 (2011), 677–687.

[2] C. T. Codeco , *Endemic and epidemic dynamics of cholera: the role of the aquatic reservoir*,BMC Infectious Diseases 1 (2001), 1.

[3] D.A. Sack , M. Cadoz , *Cholera vaccines.*, In Plotkin AS, Orenstein WA Vaccines Philadelphia: WB Saunders Co; 1999.

[4] D. M. Hartley, J. G. Morris Jr. and D. L. Smith, *Hyperinfectivity: A critical element in the ability of V. cholerae to cause epidemics?* , PLoS Medicine 3 (2006), 0063–0069.

[5] E. Asano, L. J. Gross, S. Lenhart and L. A. Real, *Optimal control of vaccine distribution in a rabies metapopulation model*, Math. Biosci. Eng. 5 (2008), 219–238.

[6] J. Wang, C. Modnak, *Modeling cholera dynamics with controls*,Canadian Applied Mathematics Quarterly, 19, (2011), 255-273.

[7] P. van den Driessche and J. Watmough, *Reproduction numbers and sub-threshold endemic equilibria for compartmental models of disease transmission*,Math. Biosci. 180 (2002), 29–48.

[8] R. L. M. Neilan, E. Schaefer, H. Gaff, K. R. Fister and S. Lenhart, *Modeling optimal intervention strategies for cholera*,Bull. Math. Biol. 72 (2010), 2004– 2018.

[9] R.M. Anderson , R.M. May, *Infectious diseases of humans*,Oxford: Oxford University Press; 1991.

[10] R. M. Nisbet and W. S. C. Gurney, *Modeling Fluctuating Populations*,John Wiley & Sons, New York, 1982.

[11] S. Liao and J. Wang, *Stability analysis and application of a mathematical cholera model*, Math. Biosci. Eng. 8 (2011), 733–752.

[12] T.K. Sengupta, R.K. Nandy, S. Mukhopadyay, R.H. Hall, V. Sathyamoorthy, A.C. Ghose, *Characterization of a 20-k Da pilus protein expressed by a diarrheogenic strain of non-O1/non-O139 Vibrio cholerae*, FEMS Microbiol Letters. 1998;160:183–189. doi: 10.1016/S0378-1097(98)00012-3.

[13] V. Capasso and S.L. Paveri-Fontana, *A mathematical model for the 1973 cholera epidemic in the european mediterranean region*, A mathematical model for the 1973 cholera epidemic in the european mediterranean region

[14] World Health Organization web page: www.who.org.

[15] Z. Mukandavire, S. Liao, J. Wang, H. Gaff, D. L. Smith and J. G. Morris Jr., *Estimating the reproductive numbers for the 2008-2009 cholera outbreaks in Zimbabwe*, Proc. Nat. Acad. Sci. 108 (2011), 8767–8772.

Output ที่ได้จากโครงการ

1. ได้ผลงานตีพิมพ์ในวารสารวิชาการนานาชาติ

Li-Ming Cai, Chairat Modnak, Jin Wang, "An age-structured model for cholera control with vaccination," Applied Mathematics and Computation, vol. 299, Article ID 127, 13 pages, 2017. DOI:http://dx.doi.org/10.1016/j.amc.2016.11.013 (Impact Factor 1.345 (2015))

ภาคผนวก

ประกอบด้วย

1. ผลงานตีพิมพ์ในวารสารวิชาการนานาชาติ เรื่อง

   An age-structured model for cholera control with vaccination

Applied Mathematics and Computation 299 (2017) 127–140

Contents lists available at ScienceDirect

Applied Mathematics and Computation

journal homepage: www.elsevier.com/locate/amc

An age-structured model for cholera control with vaccination☆

Li-Ming Cai[a,*], Chairat Modnak[b], Jin Wang[c]

[a] Department of Mathematics, Xinyang Normal University, Xinyang 464000, PR China
[b] Department of Mathematics, Faculty of Science, Naresuan University, Phitsanulok 65000, Thailand
[c] Department of Mathematics, University of Tennessee at Chattanooga, Chattanooga, TN 37403, USA

ARTICLE INFO

Keywords:
Cholera model
Age-structure
Stability
Optimal vaccination strategies

ABSTRACT

We formulate an age-structured cholera model with four partial differential equations describing the transmission dynamics of human hosts and one ordinary differential equation representing the bacterial evolution in the environment. We conduct rigorous analysis on the trivial (disease-free) and non-trivial (endemic) equilibria of the system, and establish their existence, uniqueness, and stability where possible. Meanwhile, we perform an optimal control study for the age-structured model and seek effective vaccination strategies that best balance the outcome of vaccination in reducing cholera infection and the associated costs. Our modeling, analysis and simulation emphasize the complex interplay among the environmental pathogen, the human hosts with explicit age structure, and the age-dependent vaccination as a disease control measure.

1. Introduction

Although regarded as one of the oldest known diseases, cholera remains a serious public health burden in those regions where poverty and poor sanitation are prevalent. The causing agent for cholera is the bacterium *Vibrio cholerae*, which is typically transmitted to human hosts through ingesting contaminated water and food [31]. The main symptom of cholera infection is profuse watery diarrhea that can lead to dehydration, drop in blood pressure, kidney failure, and possible death within days if not promptly treated. In recent years, a number of cholera outbreaks have taken place in Africa, South Asia, and South America, with annually 3–5 million cases of infection estimated by the World Health Organization (WHO) [41].

Current intervention methods for cholera include antibiotics, rehydration therapy, vaccination, and water sanitation. Antibiotic treatment for cholera is credited for saving a large number of lives, though the administration of antibiotics can quickly lead to bacterial resistance [26]. Oral rehydration using salt water, while unable to prevent cholera infection, is extremely effective for preventing death. Water sanitation, as well as improvement of infrastructure for water and hygiene, are ultimately the most useful means to combat cholera, but such control measures could be highly expensive, time consuming, and may not be available in an emergency setting of cholera outbreak. Vaccination has long been regarded as a cost-effective approach for cholera prevention, and has recently renewed interest for use in the course of a cholera epidemic [22]. In particular, WHO conditionally recommended the deployment of cholera vaccines in cholera emergency settings [43]. In Haiti, cholera vaccines were used with success during the recent cholera outbreak after a major earthquake in 2010 [33].

☆ This work supported partially by National Natural Science Foundation of China (11371305, 11671346, 14B110034), China Scholarship Council (201308410212) and Nanhu Scholars Program for Young Scholars XYNU(2016). Jin Wang was partially supported by the National Science Foundation under grant numbers 1412826, 1520672 and 1557739.

* Corresponding author.
E-mail addresses: limingcai@amss.ac.cn, liming_cai88@163.com (L.-M. Cai), jin-wang02@utc.edu (J. Wang).

http://dx.doi.org/10.1016/j.amc.2016.11.013
0096-3003/

There are, however, many important questions that remain to be answered in the design of control strategies against cholera [18]. For example, what would be the most effective means to reduce the morbidity and mortality, and what would be the optimal balance between the effects and costs of the control measures? In particular, recent studies [25,31] have shown that the susceptibility, disease risk and severity, and transmission of cholera among human hosts vary significantly by ages. As an example, it has been observed that while young children and some older people are most vulnerable to cholera, newborns seem to be protected against the infection from maternally derived immunity and the antibodies in breast milk [17]. Consequently, a concern of public health administration is whether age-based vaccination protocols can effectively reduce the infection and slow the spread of cholera, while limiting the costs of the control. To address the issue, we need a deep understanding of cholera dynamics, especially the details of age-structured transmission pattern.

Mathematical modeling, analysis, and simulation for infectious diseases have long provided useful insight toward better understanding of disease mechanisms and more effective prevention and control of disease outbreaks. Particularly, a large number of mathematical studies have been devoted to cholera (see, e.g., [2,5,8,9,14,20,23,28–30,36–40]). Among these, however, very few are concerned with age-structured dynamics of cholera. Alexanderian et al. proposed a model to investigate the impact of ages on the spread of cholera epidemics [1]. Brauer et al. analyzed an age-of-infection cholera model which includes both the infection age of human hosts and the biological age of pathogen [4]. Recently, Fister et al. formulated an age-structured model [15] that incorporates the effect of vaccination, with a distinction between symptomatic and asymptomatic infections among human hosts. Despite these efforts, detailed analysis of age-structured cholera dynamics has not been conducted, partly due to the complexity of the mathematical models.

The main objectives of this paper are to improve our present knowledge in cholera dynamics related to age structures, to mathematically clarify the concern in the design of age-based vaccination protocols, and to explore optimal vaccination strategies for cholera. To that end, we propose an age-structured cholera model that consists of four partial differential equations (PDEs) and one ordinary differential equation (ODE). We then conduct rigorous analysis on the equilibria of the system, including both trivial (disease-free) and non-trivial (endemic) equilibria, and establish their existence, uniqueness, and stability wherever possible. We next perform an optimal control study for the age-structured model and seek an optimal balance between the outcome of vaccination and the associated costs.

The remainder of this paper is organized as follows. In Section 2, we present our age-structured model as a mixed PDE–ODE system, with necessary notations and assumptions. In Section 3, we conduct a careful analysis for the disease-free (or, infection-free) equilibrium, and prove its existence, uniqueness, and local and global stabilities. Furthermore, we establish the existence and uniqueness of the endemic equilibrium. In Section 4, we construct and analyze an age-based optimal control model in terms of vaccination. We conduct extensive numerical simulations for the optimal vaccination solutions under different scenarios. Finally, we conclude the paper with some discussion in Section 5.

2. Formulation of the model

As a start, we develop a PDE–ODE coupled system to describe the age-dependent cholera dynamics. We assume that the total human population is divided into four classes: susceptible, infected, vaccinated, and recovered. Let $S(t, a), I(t, a), V(t, a), R(t, a)$ denote, respectively, the age-densities of the susceptible, infected, vaccinated, and recovered parts of the human population, where a denotes age and time t denotes time. Let $B(t)$ be the concentration of vibrios in the contaminated environment at time t. We employ a saturation incidence [9,32] in the form of $\beta(a)\frac{B(t)}{B(t)+\kappa}$ to model the force of infection from the environment, where κ is the half saturation concentration of environmental vibrio.

Transmission of cholera usually stems from the waterborne bacteria *Vibrio cholerae*, and therefore the infection occurs as a result of an effective contact between a susceptible individual and the pathogenic vibrios, reflected by the contact rate $\beta(a)$. It is well known that improvements in water supply, sanitation, food safety and community awareness of disease risks are the best means of preventing cholera. In addition, WHO [41] has suggested that oral cholera vaccines with demonstrated safety and effectiveness have recently become available. The deployment of cholera vaccines, through immunizing populations at higher risk of infection, provides an effective tool to complement those traditional measures against cholera outbreaks. Thus, we further assume that susceptible individuals are vaccinated at an age-specific rate $\psi(a)$, with a vaccine efficacy $1-\sigma$ (where $\sigma \in (0, 1]$). Infected individuals are treated and subsequently enter the recovered class at a rate $\gamma(a)$. $\mu(a)$ is the natural mortality rate of human population. Infected individuals contribute to vibrios in the aquatic environment at an age-dependent rate $\alpha(a)$ and vibrios have a reduction rate μ_b, which includes the natural death and other means of the removal of the pathogen in the environment. Since the case fatality rates for cholera generally are very low (at or below 1%) [42], we assume that the cholera-induced mortality can be neglected in this study. All these parameters take positive values. The variables, parameters and their biological interpretations are given in Table 1 and a flow diagram of the model is depicted in Fig. 1.

Based on these assumptions, the dynamics of the disease transmission are described by the following equations:

$$\frac{\partial S(t,a)}{\partial t}+\frac{\partial S(t,a)}{\partial a}=-\beta(a)\frac{B(t)}{B(t)+\kappa}S(t,a)-(\psi(a)+\mu(a))S(t,a),$$

$$\frac{\partial I(t,a)}{\partial t}+\frac{\partial I(t,a)}{\partial a}=\beta(a)\frac{B(t)}{B(t)+\kappa}(S(t,a)+\sigma V(t,a))-(\gamma(a)+\mu(a))I(t,a),$$

Table 1
Model variables, parameters and their units.

Variables	Description	Units
$S(t, a)$	Concentration of susceptible humans at age a and time t	$\frac{Humans}{day}$
$I(t, a)$	Concentration of infected humans at age a and time t	$\frac{Humans}{day}$
$V(t, a)$	Concentration of vaccinated humans at age a and time t	$\frac{Humans}{day}$
$R(t, a)$	Concentration of recovery humans at age a and time t	$\frac{Humans}{day}$
$B(t)$	Concentration of vibrios in the environment at time t	Cells/ml
$\beta(a)$	Ingestion rate of vibrios at age a	1/day
$\psi(a)$	Vaccination rate at age a	1/day
$\mu(a)$	Natural mortality rate at age a	1/day
$\gamma(a)$	Recovery rate at age a	1/day
$\alpha(a)$	Rate of human contribution to vibrios at age a	1/day
κ	Half-saturation concentration	Cells/ml
σ	The reduction of vaccine efficacy	None

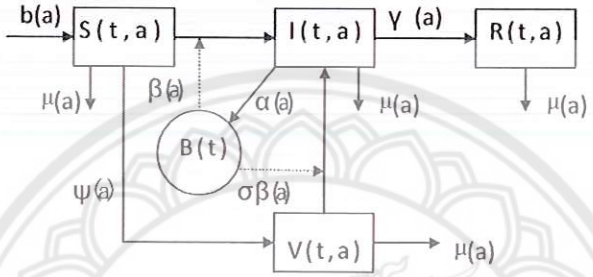

Fig. 1. The flow diagram of the model (2.1).

$$\begin{aligned}
&\frac{\partial V(t,a)}{\partial t}+\frac{\partial V(t,a)}{\partial a}=\psi(a)S(t,a)-\sigma\beta(a)\frac{B(t)}{B(t)+\kappa}V(t,a)-\mu(a)V(t,a),\\
&\frac{\partial R(t,a)}{\partial t}+\frac{\partial R(t,a)}{\partial a}=\gamma(a)I(t,a)-\mu(a)R(t,a),\\
&\frac{dB(t)}{dt}=\int_0^\infty \alpha(a)I(t,a)da-\mu_b B(t).
\end{aligned} \tag{2.1}$$

We assume that all individuals are born susceptible and unvaccinated. The boundary and initial conditions for system (2.1) are given by

$$\begin{aligned}
&S(t,0)=\int_0^\infty b(a)(S(t,a)+I(t,a)+R(t,a)+V(t,a))da,\\
&I(t,0)=V(t,0)=R(t,0)=0,\ \ S(0,a)=S_0(a),\ \ I(0,a)=I_0(a),\\
&V(0,a)=V_0(a),\ \ R(0,a)=R_0(a),\ \ B(0)=B_0.
\end{aligned} \tag{2.2}$$

where $b(a)$ is the age-specific per capita fertility rate. The initial age distributions are assumed to be known, and their values become zero beyond some maximum age.

Remark 1. We notice that Alexanderian et al. [1] also proposed an age-structured dynamical system for cholera. Like the model of Alexanderian et al., we have employed a saturation incidence here to model the force of infection from the environment. However, we have also added a vaccinated compartment, and vaccinated individuals can be re-infected due to the imperfect vaccination efficacy. Hence, our model leads to cholera dynamics that are substantially different from those of the model by Alexanderian et al. Additionally, the authors of [1] did not analyze the disease threshold, whereas we will perform a detailed study of the threshold dynamics, characterized by the reproductive number, in next section.

Let $P(t, a) = S(t, a) + I(t, a) + R(t, a) + V(t, a)$. It is straightforward to observe that

$$\begin{cases}
\dfrac{\partial P(t,a)}{\partial t}+\dfrac{\partial P(t,a)}{\partial a}=-\mu(a)P(t,a),\\
P(0,t)=\displaystyle\int_0^\infty b(a)P(t,a)da,\\
P(0,a)=P_0(a),
\end{cases} \tag{2.3}$$

This is the standard age-structured Mckendrick-Von Foerster equation [21]. The following hypotheses are necessary for analyzing this problem:

$$b(a) \in L^{\infty}(0,\infty), b(a) \geq 0 \text{ in } [0,\infty), \ \bar{b} = \sup_{a\in[0,\infty)} b(a),$$

$$\mu(a) \in L^{1}_{loc}[0,\infty), \ \mu(a) > 0 \text{ in } [0,\infty), \ \int_0^{\infty} \mu(a)da = \infty.$$

Using methods in the book [21], we assume that the net reproductive rate of the population is equal to unity and that the total population is at an equilibrium. This means that

$$\int_0^{\infty} b(a)e^{-\int_0^a \mu(\tau)d\tau}da = 1.$$

Thus,

$$P(a,t) = P_{\infty}(a) = b_0 \exp\{-\int_0^a \mu(\tau)d\tau\}, \quad \text{for all } t.$$

Therefore, for system (2.1), we chose the following the initial data

$$S_0(a) \geq 0, \ I_0(a) \geq 0, \quad V_0(a) \geq 0, \ R_0(a) \geq 0.$$
$$S_0(a) + I_0(a) + R_0(a) + V_0(a) = P_{\infty}(a),$$

which yields the relation:

$$b_0 = \frac{\int_0^{\infty} P_{\infty}(a)da}{\int_0^{\infty} e^{-\int_0^a \mu(\tau)d\tau}da}.$$

It is assumed that the recovered class $R(t, a)$ are no longer active in the disease transmission. Hence the dynamics of $R(t, a)$ does not affect the evolution of $S(t, a), I(t, a), V(t, a), B(t)$, we may omit the equation for $R(t, a)$ when we study the dynamics of the disease.

By introducing the following fractions:

$$s(t,a) = \frac{S(t,a)}{P_{\infty}(a)}, \quad i(t,a) = \frac{I(t,a)}{P_{\infty}(a)}, \quad v(t,a) = \frac{V(t,a)}{P_{\infty}(a)},$$

we investigate the following normalized system

$$\begin{cases} \dfrac{\partial s(t,a)}{\partial t} + \dfrac{\partial s(t,a)}{\partial a} = -\beta(a)\dfrac{B(t)}{B(t)+\kappa}s(t,a) - \psi(a)s(t,a), \\ \dfrac{\partial i(t,a)}{\partial t} + \dfrac{\partial i(t,a)}{\partial a} = \beta(a)\dfrac{B(t)}{B(t)+\kappa}(s(t,a) + \sigma v(t,a)) - \gamma(a)i(t,a), \\ \dfrac{\partial v}{\partial t} + \dfrac{\partial v}{\partial a} = \psi(a)s(t,a) - \sigma\beta(a)\dfrac{B(t)}{B(t)+\kappa}v(t,a), \\ \dfrac{dB(t)}{dt} = \displaystyle\int_0^{\infty} \alpha(a)i(t,a)P_{\infty}(a)da - \mu_b B(t), \\ s(t,0) = 1, \ i(t,0) = v(t,0) = 0, \ s(0,a) = s^0(a), i(0,a) = i^0(a), v(0,a) = v^0(a). \end{cases} \tag{2.4}$$

The model (2.4) with the initial and boundary conditions (2.2) is well-posed and can be applied by the Banach contraction mapping principle. The proof is similar to that in Ref. [1].

3. Dynamics of the model

3.1. Equilibria and the reproduction number

We first analyze the dynamics of our cholera model described in system (2.4). For ease of presentation, we let $\kappa = 1$ (through a normalization) in this section. Introduce

$$\mathcal{F}_{\psi}(a) = \exp\left\{-\int_0^a \psi(\tau)d\tau\right\}.$$

It is easy to obtain that

$$E_0\left(s^0(a), i^0(a), v^0(a), B^0\right) = \left(\mathcal{F}_{\psi}(a), 0, \int_0^a \psi(\theta)\mathcal{F}_{\psi}(\theta)d\theta, 0\right) \tag{3.1}$$

is the disease-free (or, infection-free) equilibrium of system (2.4).

Next, we investigate the existence of the endemic equilibrium in system (2.4). In fact, let $(s^*(a), i^*(a), v^*(a), B^*)$ be any endemic equilibrium of system (2.4). Thus we have

$$\begin{aligned}
\frac{ds^*(a)}{da} &= -\left(\frac{\beta(a)B^*}{B^*+1}+\psi(a)\right)s^*(a),\\
\frac{di^*(a)}{da} &= \frac{\beta(a)B^*}{B^*+1}s^*(a)+\sigma v^*(a))-\gamma(a)i^*(a),\\
\frac{dv^*(a)}{da} &= \psi(a)s^*(a)-\sigma\frac{\beta(a)B^*}{B^*+1}v^*(a),\\
\mu_b B^* &= \int_0^\infty \alpha(a)i^*(a)P_\infty(a)da.
\end{aligned} \tag{3.2}$$

Consequently, we find that

$$\begin{aligned}
s^*(a) &= \exp\left\{-\int_0^a\left(\frac{\beta(\tau)B^*}{B^*+1}+\psi(\tau)\right)d\tau\right\},\\
i^*(a) &= \int_0^a \frac{\beta(\eta)B^*}{B^*+1}(s^*(\eta)+\sigma v^*(\eta))\exp\left\{-\int_\eta^a\gamma(\tau)d\tau\right\}d\eta,\\
v^*(a) &= \int_0^a \psi(\xi)s^*(\xi)\exp\left\{-\int_\xi^a(\sigma\frac{\beta(\tau)B^*}{B^*+1}d\tau\right\}d\xi,\\
B^* &= \frac{1}{\mu_b}\int_0^\infty \alpha(a)i^*(a)P_\infty(a)da,
\end{aligned} \tag{3.3}$$

and

$$\begin{aligned}
1 &= \frac{1}{\mu_b}\int_0^\infty \alpha(a)P_\infty(a)\int_0^a\frac{\beta(\eta)}{B^*+1}h(B^*,\eta)\exp\{-\int_\eta^a\gamma(\tau)d\tau\}d\eta da\\
&= \int_0^\infty\int_\eta^\infty \frac{\beta(\eta)}{B^*+1}\alpha(a)P_\infty(a)h(B^*,\eta)\exp\{-\int_\eta^a\gamma(\tau)d\tau\}dad\eta\\
&=: H(B^*),\\
\text{where, } h(B^*,\eta) &= (s^*(\eta)+\sigma v^*(\eta))\\
&= \exp\left\{-\int_0^a\left(\frac{\beta(\tau)B^*}{B^*+1}+\psi(\tau)\right)d\tau\right\}\\
&\quad+\int_0^a\psi(\xi)\exp\left\{-\int_0^\xi\left(\frac{\beta(\tau)B^*}{B^*+1}+\psi(\tau)\right)d\tau\right\}\exp\left\{-\int_\xi^a\left(\sigma\frac{\beta(\tau)B^*}{B^*+1}d\tau\right\}d\xi\right..
\end{aligned} \tag{3.4}$$

From (3.4), it is clear to see that $H(B^*)$ is a strictly decreasing function of B^* with $H(0)=\Re_0(\psi)$. Hence, the equation has a unique positive root B^* provided that

$$\Re_0(\psi)=\frac{1}{\mu_b}\int_0^\infty\int_\eta^\infty[\alpha(a)\beta(\eta)h(B^*,\eta)]\exp\left\{-\int_\eta^a(\gamma(\tau))d\tau\right\}P_\infty(a)dad\eta > 1.$$

Using (3.3), we conclude that system (2.4) has a unique positive endemic equilibrium $(s^*(a), i^*(a), v^*(a), B^*)$ as long as $\Re_0(\psi) > 1$.

Thus, we have established the following result

Theorem 3.1. *System (2.4) always has the disease-free equilibrium E_0; system (2.4) has a unique endemic equilibrium $(s^*(a), i^*(a), v^*(a), B^*)$ as long as $\Re_0(\psi) > 1$.*

Remark 2. $\Re_0(\psi)$ can be regarded as the net reproduction number, introduced by Diekmann and coworkers [12], for our cholera model.

If there is no vaccination, we have $\psi(a) = 0$ and the v equation can be dropped. Denote $\Re_0 = \Re_0(0)$, and we obtain

$$\Re_0=\frac{1}{\mu_b}\int_0^\infty\int_\zeta^\infty[\alpha(a)\beta(\zeta)]\exp\left\{-\int_\zeta^a(\gamma(\tau))d\tau\right\}P_\infty(a)dad\zeta.$$

Note that $s^0(a)+\sigma v^0(a) < 1$ for all $a > 0$. Hence, $\Re_0(\psi) \le \Re_0$. This implies that when $\Re_0 = \Re_0(0) > 1$ (i.e., the reproductive number is greater than one in the absence of vaccination), a vaccination program can be used to reduce the reproductive number $\Re_0(\psi)$ to values below one. On the other hand, it can be easily verified that in the absence of age dependence, $\Re_0(\psi)$ is reduced to $\widetilde{\Re}_0=\frac{\alpha\beta(\mu+\sigma\psi)}{\mu_b(\mu+\gamma)}$, representing the basic reproduction number of the corresponding ODE system (up to a normalization factor). For our PDE system (2.4), however, the age structures of the model parameters, the initial host

distributions, and the components of the disease-free equilibrium, all play a role in shaping the reproduction number $\Re_0(\psi)$. Therefore, $\Re_0(\psi)$ can provide important information in controlling or eliminating the disease.

3.2. Stability analysis

In this section, we establish the stability results associated with the disease-free equilibrium, presented in (3.1). We first prove the following result

Theorem 3.2. *If $\Re_0(\psi) < 1$, then the disease-free equilibrium E_0 is locally asymptotically stable; if $\Re_0(\psi) > 1$, E_0 is unstable.*

Proof. To investigate the stability of the steady-state age distributions, we write

$$\begin{aligned} &s(t,a) = s^0(a) + \tilde{s}(t,a),\ i(t,a) = i^0(a) + \tilde{i}(t,a),\\ &v(t,a) = v^0(a) + \tilde{v}(t,a),\ B(t) = B^0 + \tilde{B}(t), \end{aligned} \tag{3.5}$$

for some small perturbations $\tilde{s}$, $\tilde{i}$, $\tilde{v}$ and $\tilde{B}$. Substituting (3.5) into system (2.4) and neglecting the nonlinear terms, we obtain

$$\begin{aligned} \frac{\partial \tilde{s}(t,a)}{\partial t} + \frac{\tilde{s}(t,a)}{\partial a} &= -\beta(a)\Big(\frac{B^0}{B^0+1}\tilde{s}(t,a) + \frac{1}{(B^0+1)^2}s^0(a)\tilde{B}(t)\Big) - \psi(a)\tilde{s}(t,a),\\ \frac{\partial \tilde{i}(t,a)}{\partial t} + \frac{\tilde{i}(t,a)}{\partial a} &= \frac{\beta(a)B^0}{B^0+1}(\tilde{s}(t,a) + \sigma\tilde{v}(t,a)) + \frac{\beta(a)}{(B^0+1)^2}(s^0(a) + \sigma v^0(a))\tilde{B}(t) - \gamma(a)\tilde{i}(t,a),\\ \frac{\partial \tilde{v}(t,a)}{\partial t} + \frac{\tilde{v}(t,a)}{\partial a} &= \psi(a)\tilde{s}(t,a) - \sigma\beta(a)\Big(\frac{B^0}{B^0+1}\tilde{v}(t,a) + \frac{1}{(B^0+1)^2}s^0(a)\tilde{B}(t)\Big),\\ \frac{d\tilde{B}(t)}{dt} &= \int_0^\infty \alpha(a)\tilde{i}(t,a)P_\infty(a)da - \mu_b\tilde{B}, \end{aligned} \tag{3.6}$$

with the initial and boundary conditions

$$\begin{aligned} &\tilde{s}(0,a) = s_0(a) - s^0(a),\ \tilde{i}(0,a) = i_0(a) - i^0(a),\ \tilde{v}(0,a) = v_0(a) - v^0(a),\\ &\tilde{B}(0) = B_0 - B^0,\quad \tilde{s}(t,0) = \tilde{i}(t,0) = \tilde{v}(t,0) = 0. \end{aligned}$$

Following the work of Castillo-Chavez et al. [7], we restrict to perturbations in separable form given by

$$\begin{aligned} &\tilde{s}(t,a) = \bar{s}(a)e^{\lambda t},\ \tilde{i}(t,a) = \bar{i}(a)e^{\lambda t},\\ &\tilde{v}(t,a) = \bar{v}(a)e^{\lambda t},\quad \tilde{B}(t) = \bar{B}e^{\lambda t}, \end{aligned} \tag{3.7}$$

where $\bar{B}$ is a constant. Substituting (3.7) into system (3.6), we obtain

$$\begin{aligned} \frac{d\bar{s}(a)}{da} &= -\Big(\lambda + \frac{\beta(a)B^0}{B^0+1} + \psi(a)\Big)\bar{s}(a) - \frac{\beta(a)}{(B^0+1)^2}s^0(a)\bar{B},\\ \frac{d\bar{i}(a)}{da} &= \frac{\beta(a)B^0}{B^0+1}(\bar{s}(a) + \sigma\bar{v}(a)) + \frac{\beta(a)}{(B^0+1)^2}(s^0(a) + \sigma v^0(a))\bar{B} - (\lambda + \gamma(a))\bar{i}(a),\\ \frac{d\bar{v}(a)}{da} &= \psi(a)\bar{s}(a) - \sigma\Big(\lambda + \frac{\beta(a)B^0}{B^0+1}\Big)\bar{v}(a,t) - \frac{\beta(a)}{(B^0+1)^2}s^0(a)\bar{B},\\ \bar{B} &= \frac{1}{\lambda+\mu_b}\int_0^\infty \alpha(a)\bar{i}(a)P_\infty(a)da. \end{aligned} \tag{3.8}$$

System (3.8) yields

$$\begin{cases} \bar{s}(a) = -\bar{B}\dfrac{1}{(B^0+1)^2}\displaystyle\int_0^a \beta(\eta)s^0(\eta)\exp\Big\{-\int_\eta^a(\lambda + \frac{\beta(\tau)B^0}{B^0+1} + \psi(\tau))d\tau\Big\}d\eta,\\ \bar{v}(a) = \displaystyle\int_0^a(\psi(\xi)s(\xi) - \bar{B}\frac{\beta(\xi)s^0(\xi)}{(B^0+1)^2})\exp\Big\{-\int_\xi^a\sigma\Big(\lambda + \frac{\beta(\tau)B^0}{B^0+1}\Big)d\tau\Big\}d\xi,\\ \bar{i}(a) = \displaystyle\int_0^a\Big[\frac{\beta(\zeta)B^0}{B^0+1}(\bar{s}(\zeta) + \sigma\bar{v}(\zeta)) + \frac{\beta(\zeta)}{(B^0+1)^2}(s^0(\zeta) + \sigma v^0(\zeta))\bar{B}\Big]\exp\Big\{-\int_\zeta^a(\lambda + \gamma(\tau))d\tau\Big\}d\zeta,\\ \bar{B} = \dfrac{1}{\lambda+\mu_b}\displaystyle\int_0^\infty \alpha(a)\bar{i}(a)P_\infty(a)da. \end{cases} \tag{3.9}$$

Notice that $B^0 = 0$ and $\bar{B} \neq 0$ in (3.9). Thus we obtain

$$\begin{aligned} 1 &= \frac{1}{\lambda+\mu_b}\int_0^\infty \alpha(a)\int_0^a [\beta(\zeta)(s^0(\zeta)+\sigma v^0(\zeta))]\exp\left\{-\int_\zeta^a(\lambda+\gamma(\tau))d\tau\right\}d\zeta P_\infty(a)da \\ &= \frac{1}{\lambda+\mu_b}\int_0^\infty\int_\zeta^\infty [\alpha(a)\beta(\zeta)(s^0(\zeta)+\sigma v^0(\zeta))]\exp\left\{-\int_\zeta^a(\lambda+\gamma(\tau))d\tau\right\}P_\infty(a)dad\zeta \\ &=: G(\lambda) \end{aligned} \tag{3.10}$$

Here we denote the right-hand side of Eq. (3.10) by $G(\lambda)$. Obviously, we have $G(0) = \Re_0(\psi)$.

It is clear to see that $G(\lambda)$ is a continuous function of λ. When λ is real and $\lambda \geq 0$, $G(\lambda)$ is strictly decreasing with λ, and $G(\lambda) \to 0$ as $\lambda \to \infty$. Thus if $\Re_0(\psi) > 1$, Eq. (3.10) has a positive real root for λ, and E_0 is unstable.

If $\Re_0(\psi) < 1$, a real root of Eq. (3.10) can only be negative; i.e., $\lambda < 0$. Now let $\lambda = x + iy$ be a complex root. Substituting it into Eq. (3.10), we find that the real part $x = Re(\lambda)$ satisfies the following equation

$$1 = \frac{x+\mu_b}{(x+\mu_b)^2+y^2}\int_0^\infty\int_\zeta^\infty [\alpha(a)\beta(\zeta)(s^0(\zeta)+\sigma v^0(\zeta))]\exp\left\{-\int_\zeta^a(x+\gamma(\tau))d\tau\right\}\cos y(a-\zeta)P_\infty(a)dad\zeta. \tag{3.11}$$

Since $\cos y(a-\zeta) \leq 1$ and $\frac{x+\mu_b}{((x+\mu_b)^2+y^2)} < \frac{1}{x+\mu_b}$, it follows from (3.11) that

$$\frac{1}{x+\mu_b}\int_0^\infty\int_\zeta^\infty [\alpha(a)\beta(\zeta)(s^0(\zeta)+\sigma v^0(\zeta))]\exp\{-\int_\zeta^a(x+\gamma(\tau))d\tau\}P_\infty(a)dad\zeta > 1.$$

Comparing this result with Eq. (3.10), we immediately see $x < 0$. Therefore, if $\Re_0(\psi) < 1$, the disease-free equilibrium is locally asymptotically stable. □

Theorem 3.3. *If $\Re_0(\psi) < 1$, the disease-free equilibrium E_0 is globally asymptotically stable.*

Proof. By integrating system (2.4) along the characteristic lines, we have

$$s(t,a) = \exp\left\{-\int_0^a \beta(\tau)\frac{B(t-a+\tau)}{B(t-a+\tau)+1}d\tau\right\}\exp\left\{-\int_0^a\psi(\tau)d\tau\right\}, \quad t > a, \tag{3.12}$$

which yields

$$s(t,a) \leq \exp\left\{-\int_0^a\psi(\tau)d\tau\right\}, \quad t > a. \tag{3.13}$$

Similarly, from the second and third equations in system (2.4), we obtain that

$$\begin{aligned} i(t,a) &= \int_0^a \frac{\beta(\xi)B(t-a+\xi)}{B(t-a+\xi)+1}(s(t-a+\xi,\xi)+\sigma v(t-a+\xi,\xi))\exp\left\{-\int_\xi^a\gamma(\tau)d\tau\right\}d\xi, \ t > a, \\ v(t,a) &= \int_0^a \psi(\zeta)s(t-a+\zeta,\zeta)\exp\left\{-\sigma\int_\zeta^a\beta(\tau)\frac{B}{B+1}d\tau\right\}d\zeta, \ t > a. \end{aligned} \tag{3.14}$$

From (3.13) and the second equation in (3.14), we have

$$v(t,a) \leq \int_0^a \psi(\zeta)\exp\left\{-\int_0^\zeta\psi(\tau)d\tau\right\}d\zeta, \quad t > a. \tag{3.15}$$

Substituting the first equation of (3.14) into system (2.4), we obtain

$$\begin{aligned} \frac{dB(t)}{dt} &= \int_0^\infty \alpha(a)P_\infty(a)\left[\int_0^a \frac{\beta(\xi)B(t-a+\xi)}{B(t-a+\xi)+1}(s(t-a+\xi,\xi)+\sigma v(t-a+\xi,\xi))\exp\left\{-\int_\xi^a\gamma(\tau)d\tau\right\}d\xi\right]da-\mu_bB(t) \\ &\leq \int_0^\infty \alpha(a)P_\infty(a)\left[\int_0^a \frac{\beta(\xi)B(t-a+\xi)}{B(t-a+\xi)+1}\left(\exp\left\{-\int_0^\xi\psi(\tau)d\tau\right\}\right.\right. \\ &\quad \left.\left.+\sigma\int_0^\xi\psi(\zeta)\exp\left\{-\int_0^\zeta\psi(\tau)d\tau\right\}d\zeta\right)\exp\left\{-\int_\xi^a\gamma(\tau)d\tau\right\}d\xi\right]da-\mu_bB(t) \\ &= \int_0^\infty\int_\xi^\infty \frac{\beta(\xi)B(t-a+\xi)}{B(t-a+\xi)+1}\alpha(a)P_\infty(a)\left(\exp\left\{-\int_0^\xi\psi(\tau)d\tau\right\}\right. \\ &\quad \left.+\sigma\int_0^\xi\psi(\zeta)\exp\left\{-\int_0^\zeta\psi(\tau)d\tau\right\}d\zeta\right)\exp\left\{-\int_\xi^a\gamma(\tau)d\tau\right\}dad\xi \ -\mu_bB(t). \end{aligned} \tag{3.16}$$

It can be easily shown that $\limsup_{t\to\infty} B(t) < +\infty$. Using the inequality

$$\frac{B(t-a+\xi)}{B(t)(B(t-a+\xi)+1)} \le 1,$$

and the result from (3.16), we obtain that

$$\frac{dB(t)}{dt} \le \mu_b\big(\Re_0(\psi)-1\big)B(t). \tag{3.17}$$

Thus, when $\Re_0(\psi) < 1$, from (3.17), we have $B(t) \to 0$ as $t \to \infty$. Therefore, using Eqs. (3.12) and (3.14) and the continuity of the function $B(t)$, it is now straightforward to obtain that

$$\lim_{t\to\infty} s(t,a) = s^0(a) \quad \lim_{t\to\infty} v(t,a) = v^0(a), \quad \lim_{t\to\infty} i(t,a) = 0.$$

We have thus established the global asymptotic stability of the disease-free equilibrium. □

Remark 3. Although the stability of the endemic equilibrium has not been resolved yet, our analysis and results presented in this section indicate that when $\Re_0(\psi) > 1$, a cholera outbreak will take place, and the disease will potentially persist. A critically important question, then, is how to effectively control cholera, and how to achieve the disease control with typically limited resources. Given that $\Re_0(\psi)$ strongly depends on the age structures of the host population, any cost-effective disease control measure shall take into account the age factors.

4. Optimal vaccination study

We now turn to an optimal control study of our age-structure cholera model and explore effective strategies for vaccination deployment in order to contain a cholera outbreak. We will allow the vaccination rate in our model to be both age- and time-dependent, offering more flexibility in strategic design of cholera vaccination policy in practical application. In particular, we will investigate the interplay of several factors, including the inherent age structures of a given host population, the objective of reducing total infections, and the costs of implementing vaccination, in shaping an optimal vaccination strategy.

Throughout this section, we will mostly rely on numerical simulation in our study due to the complexity of the optimal control model. Nevertheless, there have been a few standard results regarding the existence, uniqueness and optimality property of the optimal control solution. Interested readers can look into [3,10,11,13,16] and references therein for more details.

4.1. Optimal control formulation

For convenience of discussion and numerical implementation, we re-write system (2.1) as

$$\begin{aligned}
\frac{\partial S(t,a)}{\partial t} + \alpha_1\frac{\partial S(t,a)}{\partial a} &= -\beta(a)\frac{B(t)}{B(t)+\kappa}S(t,a) - (\psi(t,a)+\mu(a))S(t,a),\\
\frac{\partial V(t,a)}{\partial t} + \alpha_1\frac{\partial V(t,a)}{\partial a} &= \psi(t,a)S(t,a) - \sigma\beta(a)\frac{B(t)}{B(t)+\kappa}V(t,a) - \mu(a)V(t,a),\\
\frac{\partial I(t,a)}{\partial t} + \alpha_1\frac{\partial I(t,a)}{\partial a} &= \beta(a)\frac{B(t)}{B(t)+\kappa}(S(t,a)+\sigma V(t,a)) - (\gamma(a)+\mu(a))I(t,a),\\
\frac{\partial R(t,a)}{\partial t} + \alpha_1\frac{\partial R(t,a)}{\partial a} &= \gamma(a)I(t,a) - \mu(a)R(t,a),\\
\frac{dB(t)}{dt} &= \int_0^A \alpha(a)I(t,a)da - \mu_b B(t),
\end{aligned} \tag{4.1}$$

where the constant α_1 is introduced to balance the possibly different units between time and age; for example, $\alpha_1 = 1/365$ if we have time t in days and age a in years. We have also re-written the vaccination rate by $\psi(t, a)$, a function depending on both age and time. In addition, we have replaced the upper limit of the integral with respect to age, for practical consideration, by a finite number $A > 0$.

The initial and boundary conditions for the system (4.1) are provided in Eq. (2.2). Indeed, we have also studied another type of boundary conditions by putting all newborns into the recovered class [1]. We find that on the time scale of a typical cholera outbreak (several months to a year), the two types of boundary conditions yield very similar results.

For our study, we consider this system on an age range $[0, A]$ and a time interval $[0, T]$ for some $T > 0$. The control set is defined as

$$\Gamma = \{\psi(t,a) \in L^\infty[(0,A)\times(0,T)] \,\big|\, 0 \le \psi(t,a) \le \psi_{max}\}, \tag{4.2}$$

where ψ_{max} denotes the upper bound for the effort of vaccination. The bound reflects practical limitation on the maximum rate of vaccination that can be implemented within a given population in a given time period.

We aim to minimize the total number of infections and the costs of the control over the time interval $[0, T]$; i.e.,

$$\min_{\psi(t,a)\in\Gamma}\int_0^T\int_0^A [a_1 I(t,a) + a_2\psi(t,a)S(t,a) + a_3\psi^2(t,a)]dadt. \tag{4.3}$$

where a_1, a_2 and a_3 are appropriate cost parameters. Quadratic terms are introduced to account for nonlinear costs potentially arising at high intervention level. The minimization process is subject to the differential equations in (4.1), which we now refer to as the state equations. Correspondingly, the unknowns S, V, I, R and B are now called the state variables, in contrast to the control variable ψ. Our goal is then to determine the optimal control, $\psi^*(t, a)$ in terms of age and time, so as to minimize the objective functional in (4.3).

Following the framework in [3,13], we construct the optimal control model through the combination of the state equations, the adjoint equations, and the optimality condition. We determine the adjoint equations by first introducing the sensitivity functions. Let us denote $F = (S, V, I, R, B)$ and define the solution map: $\psi \to F = F(\psi)$. Based on results in [3], such a map is differentiable and the sensitivity functions are defined by the Gateaux derivative:

$$(Q_S,\ Q_V,\ Q_I,\ Q_R,\ Q_B) = \lim_{\epsilon\to 0}\frac{F(\psi+\epsilon l) - F(\psi)}{\epsilon},$$

for $l(a, t) \in L^\infty[(0, A) \times (0, T)]$. Consequently, the sensitivity functions satisfy the following equations:

$$\begin{aligned}
(Q_S)_t + \alpha_1(Q_S)_a &= -\beta(a)\frac{B(t)}{B(t)+\kappa}Q_S - \beta(a)\frac{\kappa S(t,a)}{(B(t)+\kappa)^2}Q_B - \mu(a)Q_S - \psi(t,a)Q_S - l(t,a)Q_S,\\
(Q_V)_t + \alpha_1(Q_V)_a &= -\sigma\beta(a)\frac{B(t)}{B(t)+\kappa}Q_V - \sigma\beta(a)\frac{\kappa V(t,a)}{(B(t)+\kappa)^2}Q_B + \psi(t,a)Q_S + l(t,a)Q_S - \mu(a)Q_V,\\
(Q_I)_t + \alpha_1(Q_I)_a &= \beta(a)\frac{B(t)}{B(t)+\kappa}(Q_S+\sigma Q_V) + \beta(a)\frac{\kappa(S(t,a)+\sigma V(t,a))}{(B(t)+\kappa)^2}Q_B - (\gamma(a)+\mu(a))Q_I,\\
(Q_R)_t + \alpha_1(Q_R)_a &= \gamma(a)Q_I - \mu(a)Q_R,\\
\frac{dQ_B}{dt} &= \int_0^A \alpha(a)Q_I\,da - \mu_b Q_B,
\end{aligned} \tag{4.4}$$

where the subscripts t and a refer to the partial derivatives with respect to time and age, respectively. Next, we introduce the adjoint variables λ_S, λ_V, λ_I, λ_R and λ_B, corresponding to the state variables S, V, I, R and B, respectively. The adjoint system (which the adjoint variables have to satisfy) is then derived by using the adjoint operator associated with the sensitivity equations presented above, together with appropriate transversality conditions and boundary conditions.

Specifically, the adjoint system is given by

$$\begin{aligned}
-\big((\lambda_S)_t + \alpha_1(\lambda_S)_a\big) &= a_2\psi(t,a) - \lambda_S\left(\beta(a)\frac{B(t)}{B(t)+\kappa} + (\psi(t,a)+\mu(a))\right)\\
&\quad + \lambda_I\beta(a)\frac{B(t)}{B(t)+\kappa} + \lambda_V\psi(t,a) + \lambda_S(t,0)b(a),\\
-\big((\lambda_V)_t + \alpha_1(\lambda_V)_a\big) &= \lambda_I\beta(a)\frac{B(t)}{B(t)+\kappa}\sigma - \lambda_V\left(\sigma\beta(a)\frac{B(t)}{B(t)+\kappa} + \mu(a)\right) + \lambda_S(t,0)b(a),\\
-\big((\lambda_I)_t + \alpha_1(\lambda_I)_a\big) &= a_1 - \lambda_I\big(\gamma(a)+\mu(a)\big) + \lambda_R\gamma(a) + \lambda_S(0,t)b(a) + \lambda_B\alpha(a),\\
-\big((\lambda_R)_t + \alpha_1(\lambda_R)_a\big) &= -\lambda_R\mu(a) + \lambda_S(0,t)b(a),\\
-\frac{d\lambda_B}{dt} &= -\lambda_B\mu_b(t) - H(t)\int_0^A \beta(a)(\lambda_S S - \lambda_I(S+\sigma V) + \lambda_V\sigma V)da,
\end{aligned} \tag{4.5}$$

where

$$H(t) = \frac{\kappa}{(B(t)+\kappa)^2}.$$

The transversality conditions are

$$\lambda_S(T,a) = \lambda_V(T,a) = \lambda_I(T,a) = \lambda_R(T,a) = \lambda_B(T) = 0,$$

for $a \in (0, A)$, and the boundary conditions are

$$\lambda_S(t,A) = \lambda_V(t,A) = \lambda_I(t,A) = \lambda_R(t,A) = 0,$$

for $t \in (0, T)$.

The characterization of the optimal control follows from standard optimality procedure, and the existence and uniqueness of the optimal solution are established from Ekeland's principle [13]. Specifically, the optimality condition is found as

$$\psi^*(t,a) = \max[0, \min(\overline{\psi}(t,a),\ \psi_{max})], \tag{4.6}$$

Table 2
Model parameters and values.

Parameter	Symbol	Value	Source
Maximum age	A	72 years	[1]
Natural mortality rate	$\mu(a)$	0.01619/365/day	[15]
Reduction rate for vibrios	μ_b	1/30/day	[9]
Vaccine efficacy	$1-\sigma$	0.7	[43]
Rate of human contribution to vibrios	$\alpha(a)$	8 cells/(day· ml)	[9]
Half-saturation concentration	κ	10^6 cells/ml	[24]
Recovery rate	$\gamma(a)$	1/5/day	[20]
Maximum vaccination rate	ψ_{max}	70%/day	Assumed
Time frame	T	100 days	Assumed

where

$$\overline{\psi}(t,a)=\frac{(\lambda_S-\lambda_V-a_2)S(t,a)}{2a_3} \tag{4.7}$$

is determined through differentiation of the objective functional with respect to the control.

4.2. Numerical settings

Our optimal control problem consists of the state system (4.1), the adjoint system (4.5), and Eq. (4.6) to characterize the optimal control. Such a problem has to be solved numerically, due to the strong nonlinearity and the coupling between the state and adjoint equations. Since our main interest here is the biological finding, we have applied first-order finite difference methods to solve the PDEs involved, for simplicity in numerical set-up and ease of code development.

Our numerical approach is based on an extension of the forward–backward sweep method [27], originally proposed for ODE optimal control simulation. Our numerical procedure consists of the following steps: first, the state equations in (4.1) are solved using a method based on forward difference in time and backward difference in age, with an initial guess for the control variable. Second, the adjoint equations in (4.5) are solved by backward difference in time and forward difference in age, using the solutions of the state equations. Next, the control is updated with the new values of the state and adjoint solutions. This process is then repeated until the convergence is achieved.

To carry out the numerical simulation, we list the values for various model parameters in Table 2.

We have conducted the numerical simulation using a Matlab code. We have found that with a time stepsize of 0.01 and age stepsize of 0.1, it takes about 30–40 min for a typical simulation on a personal computer with MS Windows 10 Professional 64-bit operating system, 1.90GHz CPU, and 4.00 GB RAM.

We use the age-dependent contact rate (i.e., rate of ingesting vibrios from the contaminated environment) proposed in [15]:

$$\beta(a)=\begin{cases}0, & 0\le a\le 2,\\ 0.3a-0.6, & 2<a\le 7,\\ -0.169a+2.683, & 7<a\le 15,\\ 0.06a-0.75, & 15<a\le 25,\\ -0.016a+1.152, & \text{otherwise.}\end{cases} \tag{4.8}$$

This formula assumes that newborns are protected from maternally derived immunity and the antibodies in breast milk, up to two years. It is also assumed that older people have smaller chances of catching the vibrios than younger people, due to their relatively lower levels of activities (which may include, among others, working or playing near aquatic environments, collecting water for household use, and preparing food) than those of the younger people. The rate of contacting vibrios is assumed to decrease as the age increases (for $a>25$).

Meanwhile, the initial age distributions are prescribed by

$$S(0,a)=\begin{cases}450a, & 0\le a\le 2,\\ -0.38198a^2+17.08376a+867, & \text{otherwise}\end{cases}$$

and

$$I(0,a)=0.02S(0,a),\qquad B(0)=0.001\kappa\,.$$

In addition, the fecundity function b, in units of years, is modeled as [1]:

$$b(a)=\begin{cases}\frac{1}{5}\sin^2\left(\left(\frac{a-15}{30}\right)\pi\right), & 15<a<45;\\ 0, & \text{otherwise.}\end{cases} \tag{4.10}$$

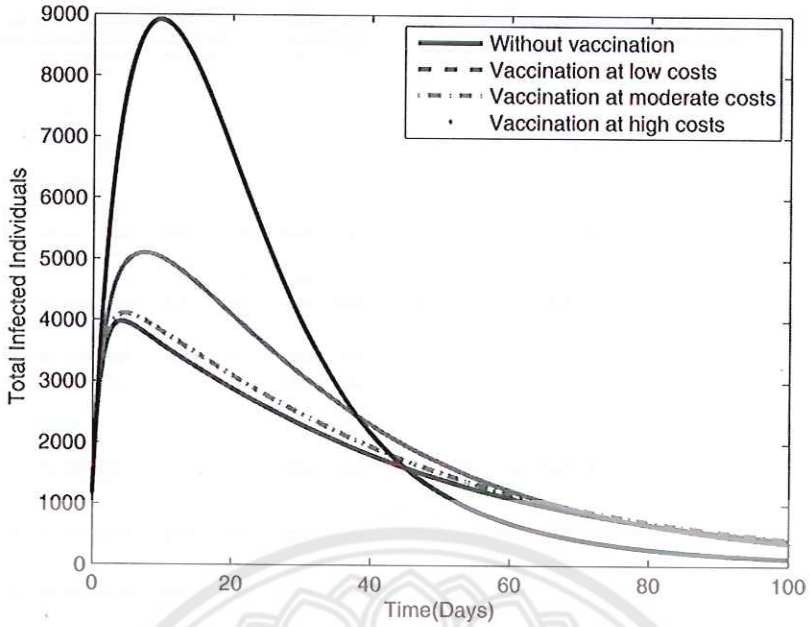

Fig. 2. The total numbers of infected individuals with and without vaccination. The parameter values are $a_1 = 500$, $a_2 = 1$ and $a_3 = 1$ for the case with low vaccination costs, $a_1 = 500$, $a_2 = 10$ and $a_3 = 100$ for the case with moderate vaccination costs, and $a_1 = 500$, $a_2 = 100$ and $a_3 = 1000$ for the case with high vaccination costs. (For interpretation of the references to color in this figure, the reader is referred to the web version of this article.)

Based on this formula, we have $\int_0^A b(a)da = 3$ for any $A > 45$. It is assumed that on average, each woman in a given host population attacked by cholera (typically in a developing country) will give birth to 3 children during the age frame $15 \leq a \leq 45$.

4.3. Simulation results

As can be naturally expected, the costs of vaccination have strong impact on the optimal control strategy. Thus we have considered three different scenarios in our numerical simulation.

The first scenario we are concerned with is $a_1 \gg a_2, a_3$; that is, reducing the number of the infected cases carries a much higher weight than that for the costs of the control in the objective functional (4.3). For illustration, we assign the values of the parameters as $a_1 = 500$, $a_2 = 1$, and $a_3 = 1$. The second scenario we are interested in has increased vaccination costs. For demonstration, we consider the case with $a_1 = 500$, $a_2 = 10$ and $a_3 = 100$. The third scenario we consider is a case with very high vaccination costs at both the linear and nonlinear levels. For illustration, we set $a_1 = 500$, $a_2 = 100$ and $a_3 = 1000$. In what follows, we refer to these three cases as scenarios with low, moderate, and high vaccination costs, respectively.

Fig. 2 compares the total infections of all ages for the case without vaccination (shown in black solid line); i.e., $\psi(0, a) = 0$, and those with the optimal vaccination strategy implemented under the three different parameter settings (with low, moderate, and high vaccination costs, respectively). We clearly see that, compared to the case with no vaccination, the number of infections has been reduced for all the three vaccination scenarios. The improvement is most significant for the case with low vaccination costs (shown in blue dashed line), where the peak value of the outbreak has been reduced from 9000 to 4000. The pattern is similar to the scenario with moderate costs (shown in red dash-dotted line), though it can be noticed that the peak value of the infection curve (about 4200) is slightly higher than that in the first case (about 4000), due to the weakened vaccination strength associated with the increased costs. For the third scenario that comes with high vaccination costs (shown in green dotted line), we see a notably higher disease peak (slightly above 5000), owing to the high costs that would limit the strength and duration of the vaccination.

Fig. 3 display the infection curves of several different ages for the cases without and with vaccination. We observe clear age variations from all these graphs. When there is no vaccination deployed; i.e., $\psi(0, a) = 0$, the age group with $a = 10$ exhibits the highest infection numbers among all those shown in Fig. 3(a), whereas those with $a = 1$ and $a = 60$ show the lowest infections. This pattern is consistent with the age-based contact rate prescribed in (4.8). With the optimal vaccination strategy implemented at low costs, shown in Fig. 3(b), we can see significant reduction of the number of infected individuals for most age groups, except for $a = 1$ where the infection risk is extremely low even without vaccination. Fig. 3(c) shows the infection curves of these different ages with optimal vaccination implemented at moderate costs. Again we see similar pattern with that in Fig. 3(b). One exception is the age group, $a = 60$, where the improvement from vaccination is rather moderate under this optimal control strategy. Fig. 3(d) shows the infection curves with high vaccination costs, and we can observe the following: (1) most age groups still exhibit reduced infections (of varied degrees) from the vaccination, and

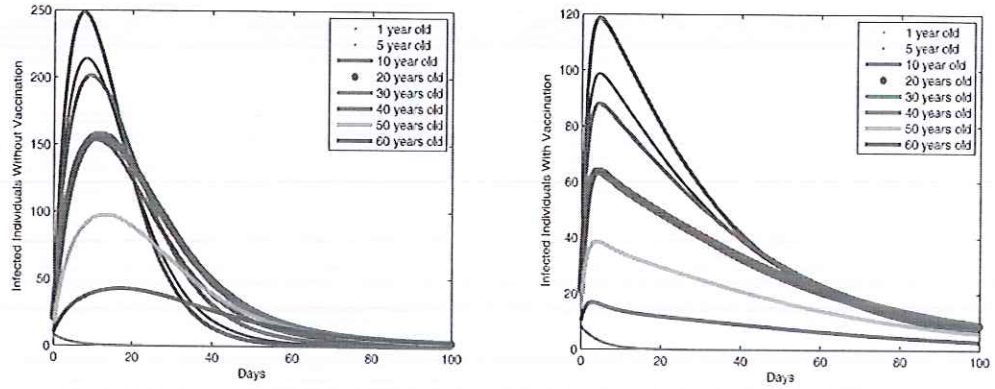

(a) Without vaccination

(b) Vaccination at low costs

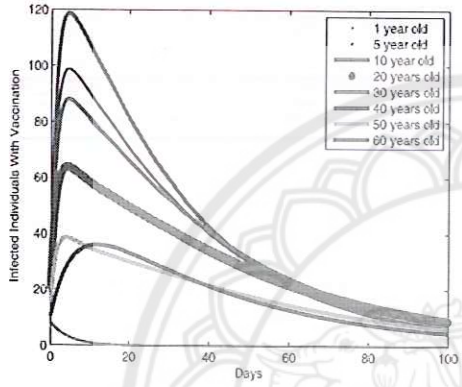

(c) Vaccination at moderate costs

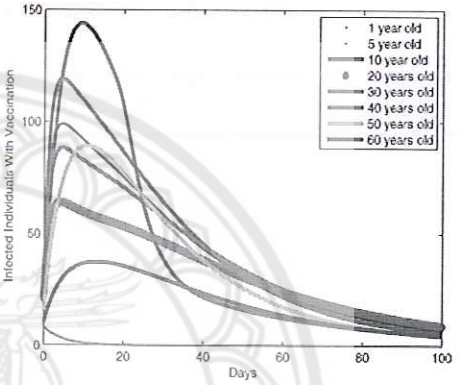

(d) Vaccination at high costs

Fig. 3. Numbers of infections by ages.

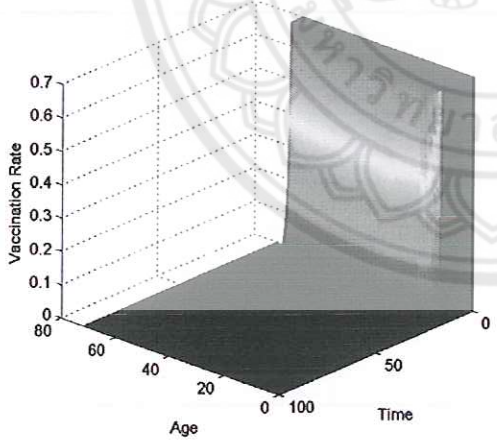

(a) Three-dimensional plot

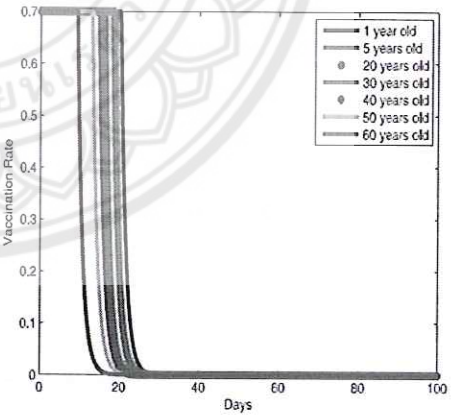

(b) Two-dimensional plot

Fig. 4. Optimal vaccination rate versus age and time.

the reduction is especially notable for those groups with higher infection risks such as $a = 5,\ 10,\ 30$ (see Fig. 3(a)); (2) a few other age groups, especially those with lower disease risks such as $a = 40,\ 50,\ 60$, appear to be receiving insufficient vaccination and thus not benefiting much from the current control strategy, a trade-off that is made to accommodate the very high costs of the control.

In addition, Fig. 4 shows the profile of the vaccination rate in its optimal balance for the case with low vaccination costs, in both three-dimensional and two-dimensional views. Such plots are natural reflections of the time- and age-dependent dynamics of our cholera model. We observe that the optimal vaccination rate varies with ages, yet, for almost all ages, the vaccination rate starts at its maximum value and remain at that level for a number of days before decreasing to lower levels of strength. Eventually the vaccination rate at all ages settles at 0.

5. Conclusions

We have presented an age-structured model to investigate the impact of ages on cholera epidemics and endemism, and to explore optimal vaccination strategies against cholera. The model is a nonlinear system with mixed PDEs and ODEs where both the mathematical analysis and optimal control simulation are nontrivial. We have rigorously proved the existence and uniqueness of the disease-free and endemic equilibria of the model, and established the basic reproduction number, $\Re_0(\psi)$, as a threshold for the age-structured disease dynamics: when $\Re_0(\psi) < 1$, the disease-free equilibrium is both locally and globally asymptotically stable, so that cholera will die out; when $\Re_0(\psi) > 1$, the disease-free equilibrium becomes unstable, and there exists a unique endemic equilibrium, indicating the outbreak, and potential persistence, of cholera.

We have also formulated and studied an age-based optimal control model in terms of vaccination, with extensive numerical simulation. Our numerical results show that vaccination can significantly reduce the disease prevalence and slow the spread of the infection, that optimal vaccination protocols are strongly dependent on ages and costs, and that strategic deployment of vaccination can effectively balance the gains and costs of the intervention. More specifically, the selection of optimal vaccination depends on several factors. First, the relative weights between the outcome (i.e., the reduction of infected cases) and the costs (i.e., the expenses related to the vaccination deployment) have to be balanced. Thus, with low costs of the control, the disease outbreak can be contained at a low level, while with increased costs, the reduction of infections will be discounted. Meanwhile, the specific age structures of the host population, involving the age distribution and time evolution, the age-dependent susceptibility, and the age-based contact pattern, etc., will have strong impact on the optimal control. Furthermore, we mention that another approach for optimal vaccination analysis is to reduce the reproductive number of the epidemic model through a vaccination strategy that minimizes the costs [6,19,35]. Compared to this approach, our optimal control model is more computationally oriented, which allows us to explicitly incorporate many different factors for a systematic investigation.

A limitation in this study is that our model has only considered the indirect (or, environment-to-human) transmission route, while several previous studies [29,34,36,37] have shown that direct (or, human-to-human) route also plays an important role in shaping cholera epidemics and endemism. Incorporating both transmission pathways into the age-structured model will possibly yield more insight into the complex cholera dynamics, but will also necessitate some non-trivial changes of the analysis presented in this work. In addition, our model and optimal control study have focused on vaccination as the disease control measure. Other intervention methods, such as antibiotics and water sanitation, can be added to the model and investigated in a similar way. A modeling framework incorporating such a holistic intervention approach might be able to provide more realistic guidance on cholera control to public health administrations.

Acknowledgments

The authors thanks the handling editor and three anonymous reviewers for their valuable comments and suggestions that led to significant improvement of the manuscript.

References

[1] A. Alexanderian, M.K. Gobbert, K.R. Fister, H. Gaff, S. Lenhart, E. Schaefer, An age-structured model for the spread of epidemic cholera: analysis and simulation, Nonlinear Anal. Real World Appl. 12 (2011) 3483–3498.
[2] J.R. Andrews, S. Basu, Transmission dynamics and control of cholera in Haiti: an epidemic model, Lancet 377 (2011) 1248–1255.
[3] V. Barbu, Mathematical Methods in Optimization of Differential Equations, Kluwer Academic Publishers, Dordrecht, 1994.
[4] F. Brauer, Z. Shuai, P. van den Driessche, Dynamics of an age-of-infection cholera model, Math. Biosci. Eng. 10 (2013) 1335–1349.
[5] V. Capasso, S.L. Paveri-Fontana, A mathematical model for the 1973 cholera epidemic in the European Mediterranean region, Rev. Epidemiol. Sante Publique 27 (1979) 121–132.
[6] C. Castillo-Chavez, Z. Feng, Global stability of an age-structure model for TB and its applications to optimal vaccination strategies, Math. Biosci. 151 (1998) 135–154.
[7] C. Castillo-Chavez, H.W. Hethcote, V. Andreason, S.A. Levin, W. Liu, Epidemiological models with age structure, proportionate mixing, and cross-immunity, J. Math. Biol. 27 (1989) 233–258.
[8] D.L. Chao, M.E. Halloran, I.M. Longini, Vaccination strategies for epidemic cholera in Haiti with implications for the developing world, Proc. Natl. Acad. Sci. 108 (2011) 7081–7085.
[9] C.T. Codeço, Endemic and epidemic dynamics of cholera: the role of the aquatic reservoir, BMC Infect. Dis. 1 (2001) 1.
[10] R.D. Demasse, J.-J. Tewa, S. Bowong, Y. Emvudu, Optimal control for an age-structured model for the transmission of hepatitis B, J. Math. Biol. 73 (2016) 305–333.
[11] W. Ding, W. Hrynkiv, X. Mu, Optimal control applied to native-invasive species competition via a PDE model, Electron. J. Differ. Equ. 2012 (2012) 1–18.
[12] O. Diekmann, J.A.P. Heesterbeek, J.A.J. Metz, On the definition and computation of the basic reproduction ratio in models for infectious diseases in heterogeneous populations, J. Math. Biol. 28 (1990) 365–382.
[13] I. Ekeland, On the variational principle, J. Math. Anal. Appl. 47 (1974) 324–353.
[14] S.M. Faruque, I.B. Naser, M.J. Islam, A.S.G. Faruque, A.N. Ghosh, G.B. Nair, D.A. Sack, J.J. Mekalanos, Seasonal epidemics of cholera inversely correlate with the prevalence of environmental cholera phages, Proc. Natl. Acad. Sci. 102 (2005) 1702–1707.

[15] K.R. Fister, H. Gaff, S. Lenhart, E. Numfor, E. Schaefer, J. Wang, Optimal control of vaccination in an age-structured cholera model, in: Chowell Gerardo, M. James Hyman (Eds.), Chapter 14 in Mathematical and Statistical Modeling for Emerging and Re-emerging Infectious Diseases, Springer, 2016, pp. 221–248.
[16] K.R. Fister, S. Lenhart, Optimal control of a competitive system with age-structure, J. Math. Anal. Appl. 291 (2004) 526–537.
[17] R.I. Glass, A.M. Svennerholm, B.J. Stoll, M.R. Khan, K.M. Hossain, M.I. Huq, J. Holmgren, Protection against cholera in breast-fed children by antibodies in breast milk, N. Engl. J. Med. 308 (1983) 1389–1392.
[18] Y.H. Grad, J.C. Miller, M. Lipsitch, Cholera modeling: challenges to quantitative analysis and predicting the impact of interventions, Epidemiology 23 (2012) 523–530.
[19] K.P. Hadeler, J. Muller, Vaccination in age structured populations II: optimal vaccination strategies, in: V. Isham, G. Medley (Eds.), Models for Infectious Human Diseases: Their Structure and Relation to Data, Cambridge University, Cambridge, 1996.
[20] D.M. Hartley, J.G. Morris, D.L. Smith, Hyperinfectivity: a critical element in the ability of V. cholerae to cause epidemics? PLoS Med. 3 (2006) 63–69.
[21] M. Iannelli, Mathematical Theory of Age-Structured Population Dynamics, in: Applied Mathematics Monographs, vol. 7, Consiglio Nazionale delle Ricerche, Pisa, 1995.
[22] M. Jeuland, J. Cook, C. Poulos, J. Clemens, D. Whittington, Cost effectiveness of new generation oral cholera vaccines: a multisite analysis, Value Health 12 (2009) 899–907.
[23] R.I. Joh, H. Wang, H. Weiss, J.S. Weitz, Dynamics of indirectly transmitted infectious diseases with immunological threshold, Bull. Math. Biol. 71 (2009) 845–862.
[24] J.B. Kaper, J.G. Morris, M.M. Levine Jr., Cholera, Clin. Microbiol. Rev. 8 (1995) 48–86.
[25] A.A. King, E.L. Ionides, M. Pascual, M.J. Bouma, Inapparent infections and cholera dynamics, Nature 454 (2008) 877–880.
[26] R. Laxminarayan, Bacterial Resistance and the Optimal Use of Antibiotics, 2001, pp. 1–23. Technical Report. University of Washington.
[27] S. Lenhart, J. Workman, Optimal Control Applied to Biological Models, Chapman Hall/CRC, 2007.
[28] S. Liao, J. Wang, Stability analysis and application of a mathematical cholera model, Math. Biosci. Eng. 8 (2011) 733–752.
[29] Z. Mukandavire, S. Liao, J. Wang, H. Gaff, D.L. Smith, J.G. Morris Jr., Estimating the reproductive numbers for the 2008–2009 cholera outbreaks in Zimbabwe, Proc. Natl. Acad. Sci. 108 (2011) 8767–8772.
[30] R.L.M. Neilan, E. Schaefer, H. Gaff, K.R. Fister, S. Lenhart, Modeling optimal intervention strategies for cholera, Bull. Math. Biol. 72 (2010) 2004–2018.
[31] E.J. Nelson, J.B. Harris, J.G. Morris, S.B. Calderwood, A. Camilli, Cholera transmission: the host, pathogen and bacteriophage dynamics, Nat. Rev. Microbiol. 7 (2009) 693–702.
[32] D. Posny, J. Wang, Z. Mukandavire, C. Modnak, Analyzing transmission dynamics of cholera with public health interventions, Math. Biosci. 264 (2015) 38–53.
[33] V. Rouzier, K. Severe, et al., Cholera vaccination in urban Haiti, Am. J. Trop. Med. Hyg. 89 (4) (2013) 671–681.
[34] Z. Shuai, P. van den Driessche, Global stability of infectious disease models using Lyapunov functions, SIAM J. Appl. Math. 73 (2013) 1513–1532.
[35] H.R. Thieme, Mathematics in Population Biology, Princeton University Press, 2003.
[36] J.P. Tian, J. Wang, Global stability for cholera epidemic models, Math. Biosci. 232 (2011) 31–41.
[37] J.H. Tien, D.J.D. Earn, Multiple transmission pathways and disease dynamics in a waterborne pathogen model, Bull. Math. Biol. 72 (2010) 1502–1533.
[38] J. Wang, S. Liao, A generalized cholera model and epidemic-endemic analysis, J. Biol. Dyn. 6 (2012) 568–589.
[39] X. Wang, D. Gao, J. Wang, Influence of human behavior on cholera epidemics, Math. Biosci. 267 (2015) 41–52.
[40] X. Wang, J. Wang, Analysis of cholera epidemics with bacterial growth and spatial movement, J. Biol. Dyn. 9 (2015) 233–261.
[41] World Health Organization (WHO), 2015. web page: www.who.org.
[42] WHO Cholera-fact sheet number 107: February 2014. http://www.who.int/mediacentre/factsheets/fs107/en/, 2015.
[43] WHO position paper: cholera vaccines, Wkly. Epidemiol. Rec. 85 (2010) 117–128.